INCREASING HOSTING CAPACITY OF DISTRIBUTION SYSTEMS FOR RENEWABLE DISTRIBUTED GENERATION BY MEANS OF NETWORK RECONFIGURATION

by

Masoud Davoudi

A dissertation submitted to the faculty of
The University of North Carolina at Charlotte
in partial fulfillment of the requirements
for the degree of Doctor of Philosophy in
Electrical Engineering

Charlotte

2017

Approved by:

_____
Dr. Valentina Cecchi

_____
Dr. Julio Romero Agüero

_____
Dr. Sukumar Kamalasadan

_____
Dr. Badrul Chowdhury

_____
Dr. Mehdi Miri

_____
Dr. Maciej Noras

ABSTRACT

MASOUD DAVOUDI. Increasing hosting capacity of distribution systems for renewable distributed generation by means of network reconfiguration. (Under the direction of DR. VALENTINA CECCHI)

This work aims at allowing for increased penetration of renewable distributed generation (DG) in the power distribution system (DS). The means to achieve this goal is changing the DS topological structure, i.e. by network reconfiguration (NR). In this work, first, a method is presented to determine the maximum allowable DG capacity based on steady-state bus voltage and line current operating limits. DS meshed topology is then investigated as a potential solution to allow for an increased installed DG capacity. This is motivated by the impacts of meshed configuration on DS stiffness, which represents the relative strength of the DS at the DG Point of Interconnection (POI). A novel NR problem is then formulated to allow for higher DG penetration while maintaining operating constraints. Although conventional NR formulations include the constraint to keep a radial topology, the radiality constraint is relaxed in this work to consider both radial and meshed configurations. Moreover, in order to minimize the impacts of variable and intermittent DG output on system bus voltages, the relationship between the DS bus impedance matrix and bus voltage variations due to power output changes is derived and incorporated in the proposed NR problem formulation. Minimization of voltage variations at the POI and at remote buses of interest (e.g. voltage-sensitive loads or voltage regulating devices) are considered. The proposed NR method is then evaluated under various test cases, including different locations of DG installation, single and multi-DG cases, different DG power factors, and DS loading conditions. The presented NR scheme shows several added benefits, including robustness to system loading conditions, with consequent reduction in switching actions, and minimized operations of voltage regulating devices.

ACKNOWLEDGEMENTS

I would like to thank my advisor, Dr. Valentina Cecchi, for all her help in performing this research and developing this dissertation. I would also like to thank Dr. Romero Agüero for his valuable insights and ideas in improving the work. I would like to appreciate the committee members, Dr. Kamalasadan, Dr. Chowdhury, Dr. Miri, and Dr. Noras, for their insightful comments and for the time they dedicated to reviewing this work.

I would also like to acknowledge my wife, for her true love and standing by me through the good times and the difficulties; my daughter, whose laughter brings joy to the meaning of my life; and my family, who has always supported me through my life.

As per the financial burden of my studies, I would like to thank Dr. Valentina Cecchi for supporting me through multiple fundings, the Electrical and Computer Engineering Department at The University of North Carolina at Charlotte for supporting me with teaching assistantships, The Graduate School at UNC Charlotte for supporting me with tuition award, The Energy Production and Infrastructure Center at UNC Charlotte for providing me with research assistantship, and Quanta Technology for supporting me with internships and research assistantships.

Finally, I would also like to thank everyone who has helped me directly or indirectly in completing this work.

DEDICATION

To my beloved wife and daughter; Shohreh and Lenna.

To my dearest mother and father.

TABLE OF CONTENTS

LIST OF FIGURES

LIST OF TABLES

CHAPTER 1: INTRODUCTION

1.1   Overview

Distributed generation (DG) is becoming a prominent feature of modern distribution systems (DS). While technical objectives such as improved reliability and efficiency can be sought by injecting power locally at the distribution level, recent environmental concerns have drawn attention to renewable resources for distributed generation. Interconnecting renewable DG improves DS performance while having less environmental impacts. However, the traditional DS is already challenged by the concerns caused by conventional DG units, and now has to face the challenges of renewable resources such as their intermittency and variability.

This dissertation concentrates on such challenges, studies the state of the art, and proposes a new method to allow for higher penetration levels of renewable distributed generation, limiting the negative impacts for distribution systems.

First, it is necessary to discuss the basic ideas leading to the motivation for the work and the problem statement discussed in the next chapter. Therefore, the following topics are presented in this chapter:

- A background for the work, including:

    - A brief review of effects of distributed generation on distribution systems

    - A definition and description of of distribution system hosting capacity

    - An overview of network reconfiguration and its state of the art in distribution systems

- The dissertation organization

1.2   Background

The grid of the future is characterized by a higher level of integration of renewable distributed generation (DG), enabled by technology improvements in power electronics, protection systems, distribution automation (DA), and communication platforms. The future grid includes bi-directional flow of information and power with decentralized supply and control, which will enable active participation by customers. With the increased presence of DG, traditionally passive distribution systems have changed to active elements of the power system. Therefore, in the first part of this section, a background literature survey is presented on how the increased presence of DG has changed the characteristics and dominant features of DS in recent years.

Moreover, the technological improvements in distribution automation and communication platforms have attracted attention toward possible benefits of changing the topological structure of the DS, i.e. network reconfiguration, and the operators are more interested in controlling the behavior of distribution system using such approaches. Hence, state of the art in network reconfiguration in DS and its technical objectives are presented in the next part of this section.

1.2.1   Effects of Distributed Generation (DG) on the Distribution System (DS)

Electric power systems consist of different parts, namely generation, transmission, and distribution, with specific tasks dedicated to each of them. Traditionally, electric power is generated from bulk power plants at voltage levels around 11 kV to 25 kV. Then, this power is converted to a higher voltage level, typically higher than 120 kV, to be transmitted with the transmission system. Then, the sub-transmission system carries the power to the distribution system, which is typically of voltages lower than 69 kV. The distribution system is the final stage in the process of delivering power from generation to the end users and is the system closest to the customers [1, 2].

In the last few decades, power plants have become larger and their generation levels

have increased. Transmission systems have also been highly developed and expanded geographically to deliver power to more areas in the nation. Instead, distribution systems have historically been referred to as the unglamorous [1] part of the power system and their importance has been traditionally undervalued.

Distributed generation refers to small power generation units usually connected at the distribution voltage levels which inject energy to the distribution system locally, in comparison with the bulk power plants that generate higher amounts of electrical power. Different types of renewable energy as well as fossil fuels can be used as DG. The renewable DG refers to wind, solar, combined heat and power, hydropower, and other categories. With the advances in power electronic technologies, integrating renewable energies to the system has become easier and both utility-sized renewable DG units and small residential sized photo-voltaic (PV) systems are commonly used nowadays. Installing DG in the distribution system can have positive and negative effects on the system, and there is a need to adequately choose the permissible amount of DG penetration such that the advantages are not turned into disadvantages.

Integrating DG in the network, if properly sized and located, can have advantages for the system. Regardless of its type, a DG may increase the reliability of the power supply provided to the customers. A perspective to view this improvement is the ability of DS to locally provide a portion of its loads in presence of disturbances, and avoid overload in parts of its structure [3–6]. Some literature have even proposed keeping the DG units online in case of disturbances while operating in islanded mode to improve the DS reliability [7,8], which can lead to a reduced interruption time and faster restoration of service.

Most of power system losses are seen at the distribution level [1], mainly due to heavy currents flown through the lines and other devices. Presence of DG to generate power locally may reduce the current through the main feeder from substation to the DG location, and lead to reduction in overall system losses [9, 10].

As another benefit of DG in DS, voltage profile improvement can be mentioned. Since the power is locally generated, the voltage drop en route to the customer will be reduced, and the voltage profile may be boosted. This will in turn lead to the capacity of distribution system to withstand higher demand levels [11, 12].

Moreover, presence of DG in DS may also lead to deferment of investment [11, 13]. The reason is that the distribution system operators usually consider investment for upgrading the feeder while the operating point of the DS is close to its marginal limits. These limits might be the maximum current flow through the transformer or feeder, the minimum voltage seen in the feeder, or high power losses observed in the DS [13]. Based on the previously mentioned advantages of DG, presence of such resources may lead to better voltage profile, lower current flow in the feeder, and reduced losses, which all can be helpful to the system operator and may lead to a deferment in the required investments.

Finally, if instead of conventional energy resources for DG, renewable resources such as wind and solar are utilized, the presence of renewable DG in the system will contribute to the reduction of pollution and greenhouse gases [14, 15].

1.2.2 Distribution System Hosting Capacity

In addition to the advantages discussed in the previous section, presence of DG in DS may bring negative impacts on system performance. If the DG location and size is not selected properly, injection of power from the DG might cause overvoltages [16], and/or lead to higher power losses in the system [17]. Moreover, some renewable types of DG inject power to the system using power electronic devices, which in turn will increase the harmonic level in the system [18]. Presence of DG in the system can also interfere with the operation of voltage regulators. Some updates in the protection system may also be required, by modifying relay settings and/or changing fuses to relays or unidirectional relays to bidirectional ones. Some other concerns are related to the variability of renewable-type of generation (e.g. solar PV), or voltage

fluctuations due to the intermittent nature of some types of DG, which can cause an increased operation of voltage regulating devices or temporary overvoltages in the system [19,20]. Therefore, distribution systems can benefit from the presence of DG if sizing, location, and type of allocated DG is such that the advantages are not turned into disadvantages.

While it is desired for the DS to host DG, higher penetration levels may cause the DS to operate at its maximum available capacity. Hence, careful measures are needed such that the system and all its elements can accommodate the desired level of DG penetration without negative impacts. DG integration in DS might be limited by bus voltage and line current limits, interaction with voltage regulators and control schemes, effects on the correct operation of protection systems, and harmonic levels in the system [21–24]. As for voltages, DS bus voltages are desired to remain within specified thresholds, hence, while increasing the DG penetration, voltages should not violate the higher limit. Moreover, if the DG absorbs reactive power, the voltage might be decreased in some buses while DG penetration is increased, and the minimum steady state voltage limit should also be considered. By injecting power into the system, line currents will also change, and the penetration level should not increase line currents above their loadability limits. Although the amount of harmonic injections from DG units have been significantly decreased with the technology refinement of power electronics [25], DG harmonic injections can also be seen as a limiting factor for increasing DG penetration [26–28].

Recently, more renewable distributed generation, and specifically PV units, are present in the distribution system. Fig. 1.1, [29], shows the expected growth of PV integration in power systems through the year 2030. The residential-size renewable DG units, such as rooftop PV, try to compensate some portion of the load where they are located and will have less effects on adjacent buses. However, the impact of many residential PV units on the distribution system is significant. The impact of

utility sized PV units (larger than 1 MW) can also be significant on DS performance, and might lead to backward flow of power to the substation, increased losses, voltage violations, etc.
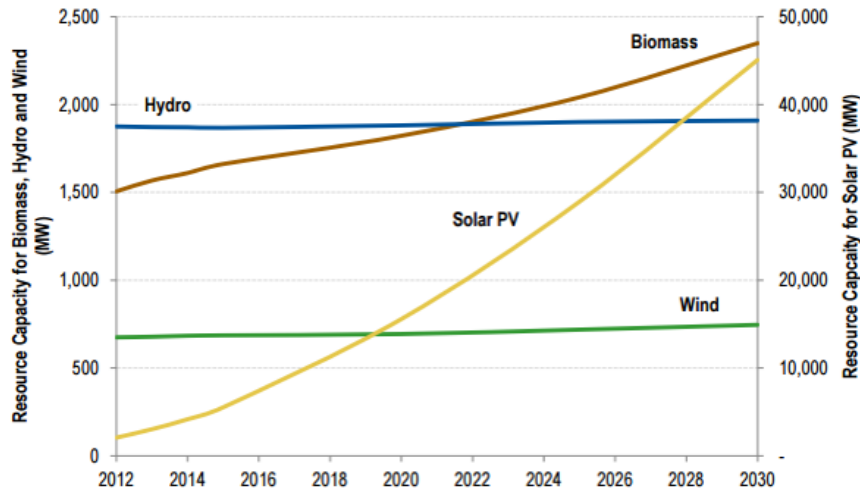
Figure 1.1: Resource capacity for PV vs. biomass, hydro and wind [29]

Hosting capacity of a feeder is defined as the maximum DG output that the feeder can accommodate without experiencing adverse impacts [30, 31]. This capacity depends on the DG type, feeder characteristics, limiting criteria defined by the operator (such as voltage and loading limits), operation of voltage regulating devices, protection system, whether it is assesses locally or for the total system, etc. For example, [22] presents an exhaustive method to determine hosting capacity of DS based on maximum allowable voltage fluctuation In [31], steady-state voltage and current limits as well as some protection aspects are considered. In order to assess DS hosting capacity, steady-state bus voltages are considered in [32], and harmonic distortion is used in [18, 27].

Recently, more PV units are present in the DS. Intermittent renewable DG units may cause higher variation in bus voltages and hence affect system operation negatively, and would require specific mitigation strategies [33]. Specifically, a more important concern for the industry is utility-size renewable DG and PV units (larger than

1 MW), since they can have more contribution to increased losses, voltage violations, etc. This work focuses on increasing the hosting capacity of DS while considering the variable nature of renewable resources such as PV.

1.2.3   Distribution System Network Reconfiguration (NR)

Network reconfiguration (NR) is changing the topological structure of the DS by closing/opening normally open (NO or tie) and normally closed (NC or sectionalizing) switches to obtain desired goals by the operators. NR can be performed to achieve different technical goals such as voltage profile improvement, power losses reduction, reliability improvement, network restoration, etc. [34,34,35,35–47], while some limiting criteria might need to be considered as well; steady-state voltage limits and line currents, and satisfying the load and generation equity are among the most commonly seen limiting criteria, referred to by normal operating limits. Furthermore, NR can be done in a static or dynamic manner. Static reconfiguration is a snapshot-based scheme which finds a fixed topology with improved performance at the planning stage. This can be done for a snapshot of load, like minimum or maximum loading conditions. When considering PV-DG in the system, one can consider the annual minimum and maximum load of a distribution system at noon (when the PV output is expected to be maximum) as a worst-case scenario and perform the studies to validate the proposed NR scheme. Dynamic reconfiguration on the other hand, considers the variability of load as well as that of DG (if variable DG is present), and focuses on a longer time horizon. While dynamic reconfiguration can be done for planning, given the required computational speed of the proposed NR scheme, the communication platform, and benefiting from the switches with remote-control capability, dynamic reconfiguration can be converted to an on-line operation scheme to pursue the desired goals in real time [34]. In this case, control signals can be sent to the switches to do even an hourly NR to pursue desired goals [35]. The latter benefit of dynamic NR is investigated in the context of future active/smart grids.

Static reconfiguration is used widely in the literature. In [36], power losses are minimized while other objectives such as voltage improvement and minimizing the number of switching operations are also considered. Load profile is considered constant and DGs are not considered in the study. [37] also minimizes power losses considering constant load profile, without taking DGs into consideration. In [38], minimizing the losses and switching costs are considered, again with constant load profile and without DG presence. In [39], minimizing power losses as well as improving voltage profile and power quality are focused, with same assumptions on load and DG. In [40], voltage sags are optimized in the presented static NR scheme, while DG presence in the DS is also considered; however, both load and DG profile are considered constant. In [41], power losses are minimized using a static NR scheme.

Dynamic NR has also been presented in the literature. Dynamic implementation of the proposed scheme in [41] is also investigated, where resolution of load and PV profile are 15 minutes and 1 hour, respectively, and PV units are set at unity power factor. In [42], the idea that NR can be used in case of abnormal conditions to overcome the impacts of outages and contingencies is discussed, and the presented NR approach has considered minimizing the overall operation costs, including switching as well as demand and wind curtailment costs. Resolution of load and DG data is 10 minutes. [34] presents a NR framework where the main optimization goal is increased hosting capacity of DS. The presented framework also considers both static and offline dynamic NR options for planning purposes. Load and wind profiles have hourly resolution. In [43], a long-term offline dynamic NR scheme is presented for power system planning which aims at improving power losses and voltage profile. Hourly load profile is considered, while DG profile is constant. [35] discusses the potential benefits of hourly dynamic NR scheme in the presence of renewable energy resources to minimize daily power losses while switching cost is also considered. Hourly resolution is considered for the renewable resources and the load profile. Voltage profile, power

losses, and switching operations are optimized using NR and reactive power dispatch from RDG units in [44]. The paper suggests that with the use of proper communication platform and real time measurements in DS, a switching schedule for optimum NR can be achieved even in presence of variable load and DG output. The daily load and DG profiles are investigated in 6 periods, resulting in very smooth variations in their profiles. [45] presents an optimal location and sizing of DGs and energy storage systems (ESS) in order to minimize the total costs of investment, maintenance, emissions, unserved power, and energy generation. The paper also discusses how NR can highlight the benefit of ESS and DG allocation form this perspective. Data resolution for load and DG output is one hour.

The number of switching operations is an important feature in network reconfiguration. In static NR scheme, it is calculated by the total changes in the status of NC and NO switches from the base configuration to the optimal topology. In dynamic NR schemes, it is the summation of changes in switches' status during the study period. Some papers, such as [37,38,40–42] have not discussed the resulting number of switch operations in their work. The NR scheme presented in [43] has led to an average of 4 switching operations per day in order to improve losses, while only constant DG is present in the DS. The method in [35] needs a total of 72 switch operations per day to minimize losses, which considering that the test system has 33 buses, and resolution of load and renewable resources is 1 hour, seems significant. The NR scheme in [44] needs an average of almost 30 switching operations per day to minimize losses and improve voltage profile in the IEEE 33 bus system, while data resolution of load and renewable resources is 4 hours. Limiting the number of switching operations is of great importance for DS operators, since too many switch operation will reduce the expected life-time of the switches. The proposed NR schemes in this work are more robust to the variations of load and DG profile, which will reduce the required number of switching operations to achieve the desired goal of the presented methods. More-

over, the presented schemes can yet consider the limitations on switch operations, and the DS operator can choose the optimum topology while limiting the switching operation to a desired limit.

1.3   Organization of Dissertation

This dissertation is organized as follows:

- In Chapter 2, mitigation strategies for increased presence of distributed generation are discussed. Then, meshed topology of DS, which is achieved with a relaxed radiality constraint for network reconfiguration, is discussed and its advantages and challenges are studied. Finally, the motivation for the work and a summary of proposed contributions are provided.

- In Chapter 3, a method is presented to calculate the maximum allowable DG power output in distribution systems, while considering both steady-sate voltage and current criteria in the system.

- In Chapter 4, expected changes in maximum allowable DG penetration while reconfiguring the DS are studied; DS meshed configuration is then studied for possible improvement of DS hosting capacity using the method presented in Chapter 3.

- Chapter 5 considers the variable and intermittent nature of renewable DG and presents equations which can relate such behavior to the changes in voltage profile. These equations are then analyzed and confirmed using a popular test case.

- Chapter 6 presents a generalized NR scheme for increased penetration of DG considering steady-state current and voltage limits, while taking the variable renewable DG profile into account. Different case studies have been performed

in both steady-state and dynamic simulation platforms to assess the behavior of the achieved DS configuration with respect to the desired objectives.

CHAPTER 2: PROBLEM STATEMENT

2.1   Overview

The need for upgrading distribution system infrastructure in order to host more distributed generation was discussed in the previous chapter. In this chapter, first, various strategies for increased DG penetration are studied and their advantages and challenges are discussed. Then, state of the art in meshed operation of DS is presented. Finally, the motivation of this dissertation and the summary of proposed contributions are discussed in the last subsection.

2.2   Strategies for Increased Penetration of DG in DS

As stated earlier, along with several benefits, distributed generation might bring challenges to the operation of distribution systems. In brief, a conventional (non-intermittent and renewable) kind of DG can increase voltages and currents in the system, and even careful planning and calculation for proper sizing and location of DG installation might lead to overvoltages and overcurrents. As a general approach, if both technically and economically possible, the distribution system can be reinforced to withstand the desired level of DG penetration. This might include replacing distribution lines, transformers, fuses and breakers, etc, which is denoted by DS reinforcement. Tackling side-effects of high penetration of DG would be even more challenging when renewable DG is being considered, due to its different nature and its impact on system operation. More specifically, renewable DG such as PV, have variable and intermittent output due to the nature of sun irradiance and other effects such as clouding. This variable and intermittent output can cause voltage variations, over and/or under voltages, and increased operation of voltage regulator.

Since capital investment in reinforcing the DS is costly, other techniques to mitigate the negative effects of increased DG penetration are of high interest to system operators and planners. Current proposed solutions to the increased renewable DG presence in DS typically imply modifying operation settings of existing components (e.g. line voltage regulators and capacitor banks), using smart power electronic devices or energy storage systems, and controlling the reactive power consumption/injection of the DG.

A solution to intermittent behavior of renewable resources is to use energy storage systems to increase the reliability and controllability of the system. There are different energy storage technologies that can be used, and the energy management system can follow different objectives [48–52]. Among different energy storage technologies, battery energy storage systems (BESS) have been used recently to allow for proliferation of renewable resources in the system for better control and with added functionalities. For instance, BESS is shown to improve reliability of the smart grid in the presence of PV-DG and wind generation units, as well as other benefits to the system operator. BESS can also be advantageous for mitigating the fluctuating nature of PV and wind generation [53, 54]. In [55], an active management strategy is proposed to optimize hosting capacity of distribution systems through a cost-benefit analysis for wind energy curtailment. In [56], a multi-objective framework for optimal placement and capacity allocation of the wind farms is proposed to maximize DS hosting capacity and minimize the energy procurement costs in a wind integrated power system, viewed from a planning perspective. Another solution usually sought by the industry is changing the power factor of the DG output using smart inverters [57–61]. Impact of different DG power factors will be studied later in this dissertation; however, in brief, absorbing reactive power by DG will pave the way for higher active power output from the DG unit. Several researches in the literature have used this technique directly or implicitly. For instance, [57, 59] have discussed the use of active

and reactive power control of PV-DG inverter systems for increasing hosting capacity.

The aforementioned solutions have their own side effects; BESS might not be effective for very high penetration level of utility-size DG. This is due to the additional costs of maintenance and operation of BESS, and the fact that larger size of BESS will be required for high penetration levels of DG, which will in turn increase the operation costs. In [55], although energy management concept is used for increased hosting capacity of DS, a cost is associated with curtailment of energy since DG is not utilized to its full potential. With respect to he use of inverters to control the power factor of DG [57, 59], regardless of the additional cost imposed to the operator, technical reports have shown practical difficulties in applying such techniques [62]. All previously mentioned solutions for integrating higher DG into the DS are valuable contributions. It is indeed desirable to not only use these solutions, but also try to move toward a more robust mode of operating the DS with increased self-ability to withstand and host higher DG presence, which is the focus of this dissertation.

2.3   Network Reconfiguration with Relaxed Radiality Constraint: DS Meshed Configuration

In all cited literature for network reconfiguration, the DS is operated radially. Historically, especially in the United States, suburban and rural distribution systems have been designed and operated in a radial manner, which are characterized by unidirectional flow of power from the substation to each customer. Radial configuration has been predominant due to its simple and economical operation and protection requirements. However, this configuration has evident efficiency and reliability shortcomings. A fault disconnection would discontinue the service to all downstream loads. Moreover, this configuration causes significant voltage drop along the feeder, and has higher power losses. In order to increase the reliability of the radial configuration, normally open tie-switches and normally closed circuit breakers have been used. In case of a fault, these switches would change their states and the continuity of service

would be held.

Nowadays, with the advent of smart system technologies and distribution automation, more attention has been put on intelligent power systems with the aim of increasing efficiency, stability, reliability and power quality. A smart system includes bi-directional flow of information and power, and decentralized supply and control, which will enable active participation by customers. Distribution automation refers to a system which allows for monitoring, control, and operating the distribution system remotely in a real time mode. As distribution grids evolve into highly dynamic systems, it is necessary to explore alternative operation approaches that facilitate higher penetration levels of DG.

While distribution systems are traditionally planned and operated in a radial manner, several papers have shown drawbacks of such operation, and, inspired by the transmission and sub-transmission grids, have investigated DS meshed configuration. This section presents the real world experiences and findings in the literature which have justified meshed topology. This section also reviews literature discussing methods to mitigate protection challenges brought on by the meshed topology.

2.3.1 Industrial Experiences with Meshed Configuration of DS

Real field experiences of meshed topology are reported by several utilities in Florida, Taiwan, Hong Kong, Singapore, Finland, Italy, France, the UK, Manhattan (New York City), and Brazil [63–72].

In 2000, Florida Power Company applied a closed-loop primary-voltage distribution automation system in order to improve reliability of its customers [63]. While the original configuration had four underground and two overhead 12.47-kV feeders, four new underground feeders were installed, and eight underground feeders were then connected in pairs to form four primary loops. Later, [64] and [65] have discussed findings of a consortium of 6 utilities working on implementing meshed topology to improve reliability of radial DS. These works criticize the reliability challenges faced in

a radial topology even in presence of automation and mention meshed DS as the most reliable DS configuration. [66] discusses the presence of meshed medium voltage DS in Finland for improved reliability. Another real-life implementation example of meshed topology is the three closed-loop feeders in an area with many critical customers in Taipei City, Taiwan [67,68], implemented in 2002. In [67], upgrading primary feeders from radial and open loop to a normally closed-loop (meshed) arrangement using this system as the case study has been investigated, showing superior performance of the meshed topology. [68] has mentioned that not only reliability, but also losses are improved in this practical system, and the investments on upgrading the protection system are justified. [69] has investigated meshed vs. radial topology on a real Italian distribution system, showing superior performance of the former topology. The paper also justifies that the change toward meshed topology in most cases does not require building new lines because DS are already meshed but radially managed. [70] presents a new hybrid structure of radial and meshed operation for a real French network to improve DS reliability. The method tries to minimize the total length of the conductor, which will lead to minimization of the investment cost of the network. [73], using real test cases in central England, discusses that losses can be reduced using meshed configuration. [71] discusses possible impacts of distributed generation (DG) on voltage profiles in low-voltage secondary distribution networks. A real test case of the LV secondary network in downtown Manhattan, NY, is used, where multiple loops exist in the system. More details about the test case is reported by Con Edison of New York in [74]. [75] solves an optimization problem to improve the average voltage deviations, minimize the total line losses and maximize the possible installed capacity of DGs, considering meshed configuration for the DS.

Meshed configuration has also been considered in the concept of microgrids. In [76], attention is paid to the presence of meshed microgrids and their voltage control in islanded mode of operation. In [77], drawbacks of radial DS have been mentioned, and

loop-based microgrid topology was shown to provide more opportunities to enhance the resilience and reliability of power delivery. The paper has used the real field microgrid of Illinois Institute of Technology (IIT), Chicago as its test case.

2.3.2   Meshed Configuration: Effect on Protection System

Protection of traditional DS is designed for a radial configuration, therefore, operating the DS in a meshed topology requires updates to the protection system. However, protection of radial DS is already challenged by the bi-directional flow of power caused by DGs, and the of DG alone is already pushing the need for upgrading the protection systems of DS to move toward a transmission-system-like scheme.

Real-life implementations of DS meshed configuration have proposed reliable protection schemes using advanced protection devices commonly used in transmission systems. In the real implementation reported in Florida, [63], the company has invested in upgrading the protection system in the previously exiting six feeders to be compatible with the relays in the new feeder breakers [78]. In brief, conventional overcurrent relays were replaced by directional relays operated in a pilot scheme using a fiber communication platform. The investment, costing around \$8M at the time, has proven to be worth doing. [68, 72, 79] discuss the protection system of the meshed DS case study in Taiwan [67]. The protection system is a pilot relaying scheme with a reliable fiber-optical communication channel. Although investment cost of this system is relatively expensive, it is justified by the outstanding improvement of service reliability. The proposed protection scheme is extremely well designed, and the number and the duration of interruptions are minimized. [80] first discusses a fiber-optic communication based protection scheme implemented for a radial feeder in California served by Southern California Edison(SCE). Then, radio-based communication is used instead of fiber-optic platform, and the radial feeder is reconfigured as meshed for improved reliability and reduced cost. The radio-based communication platform reduces the implementation cost, hence allows for reliable coordination of the relays

in meshed topology. As can be seen, all real life implementations have used pilot relaying schemes instead of the conventional relaying philosophies in radial feeders.

New protection schemes for DS meshed configuration are also discussed in the literature. [81] discusses the impacts of high DG penetration on protection coordination in meshed DS, and proposes a protection scheme for meshed DS to mitigate such impacts. For this purpose, the DG needs to be connected to two feeders, which are connected together in a loop structure. The protection scheme breaks up the loop in order to isolate the DG from the faulted feeder, clears the fault in the faulted feeder (which is now in radial mode), and restoring the meshed topology in case of temporary faults. This scheme needs high speed line protection relays enabled by pilot protection. [82] presents different protection schemes for meshed DS. Each scheme provides different reliability improvements; while higher reliability requires higher investments:

- The first scheme changes the meshed configuration to a radisal topology as soon as a fault happens in the loop. This system does not improve the reliability.

- The second scheme replaces all reclosers with directional overcurrent relays, and hence the interrupted load in case of a fault would be limited between two breakers.

- The third scheme replaces the directional overcurrent relays of second scheme with distance protection.

- The fourth method, which is the most expensive one, uses pilot protection to allow for instantaneous operation of distance relays for their protected area.

The paper has shown that when the feeders with DG are operated in a meshed topology, additional reliability advantages are seen in four scenarios discussed above.

[83] discusses the challenges of the four schemes presented in [82]; mentioning long fault clearing time for directional overcurrent scheme and challenges of distance

scheme due to short length of distribution lines. Then, it proposes pilot over-current protection scheme for protection of meshed DS. [84] presents a protection scheme for meshed microgrids which uses power line carrier (PLC) technology as the communication platform; hence lowering the cost of investment for implementing the scheme. In [85], the DS a "quick delooper" changes the DS meshed topology to the base configuration so that the protection system could act as it would in radial operation. In [86], pilot dual-setting directional overcurrent relays are proposed for protecting meshed DS with DG. These relays have two inverse time-current curves, and the appropriate curve would be chosen based on the direction of fault current. Comparing the proposed scheme with conventional single characteristic overcurrent relays shows higher speed of the presented method. As can be seen, the literature is also paying attention to the protection schemes used in transmission system, and the conventional overcurrent-based protection scheme of radial DS is changed to more reliable schemes.

2.4   Motivation and Summary of Proposed Contributions

As an important part of the power system, distribution systems are the closest section to the end-users with almost 100 times more components than the transmission system and a capital outlay of almost 40% of the total power system (almost twice that of the transmission system) [1]. However, less attention had been paid to this traditionally passive section of the power system until recent years, when increase in environmental concerns regarding the use of fossil fuels as well as the desire to generate power locally prompted a significant attention toward increasing the penetration levels of (mostly renewable) DG in the system. However, the traditionally radial distribution system may not be able to withstand the proliferation of DG without careful mitigations. Although some solutions have been presented to allow for higher DG penetration, aiming at modified settings of existing components in the distribution system or regulating the output of DG units, these solutions are a temporary fix to the problem, and might not work for very high penetration levels. In a general

sense, these solutions can be seen as a temporary fix to a more fundamental problem caused by the radial operation of the distribution system.

Advances in smart system technologies, DA, power electronics, and protection technologies have paved the way for exploring alternative distribution operation modes. One possible approach is forming loops in the primary distribution systems, similar to transmission lines, which is referred to as meshed configuration. Despite its complexity and concerns, this mode of operating the distribution system has several benefits. With careful planning, meshed operation of the distribution system could be such that its negative impacts are omitted or decreased, and the positive effects could be exploited.

Inspired from transmission and sub-transmission systems, forming loops in the distribution system is proposed in this work to allow for higher DG integration. The idea is originated considering different aspects of meshed configuration. First, DG integration generally happens towards the end of the feeder, or at least with some distance from the substation. The injected power from the DG will then be traveling along the lateral in which it is located, possibly causing overcurrent and overvoltage in that region. Contrary to this condition, the power can possibly flow in more lines in a meshed configuration, causing less issues than the former condition. Another idea is the relative strength of the power system at the Point of Interconnection (POI), regarded to as stiffness factor. Stiffness factor of the system, which is inversely proportional to the Thevenin impedance seen at the POI, is also typically inversely proportional to the distance from the substation. Forming loops in the distribution system can help increase this factor at the POI, and help increase the maximum allowable DG penetration level. The relationship between stiffness factor and maximum allowable DG penetration will also be discussed later in this work. Meanwhile, network reconfiguration has been presented thus far to improve the operation of distribution systems, mainly focusing on improving reliability, power losses, voltage profile

etc. In our investigations to define maximum allowable DG penetration in the DS based on steady state voltage and current, the network topology, i.e. the way buses are connected to each other, also affects this maximum value.

Hence, this work aims at proposing a generalized network reconfiguration scheme with a general formulation shown in (2.1).

$$\max_{X} \ G = \sum_{k=1}^{n_{DG}} P_{DG_k} \qquad (2.1)$$

where P_{DG_k} and n_{DG} are the active power output of the kth DG unit and the total number of DG units in the system, respectively, and X, the vector of decision variables, consists of states of the switches, S, and amount of power injection from each DG unit.

While the objective is to maximize the value of function G, there are some constraints which limit this function. The steady-state constraints to the problem are bus voltage and line current limits:

$$V^{min} < V_{bus_i} < V^{Max}, \ i = 1 \ to \ N_{bus} \qquad (2.2)$$

$$I_{line_j} < I_{line_j}^{Max}, \ j = 1 \ to \ N_{line} \qquad (2.3)$$

where N_{bus} and N_{line} are the total number of buses and lines, respectively, V^{min} and V^{Max} are the minimum and maximum allowable voltage threshold in the system, and $I_{line_j}^{Max}$ is the maximum line current limit for line j.

Considering the relationship between Thevenin impedance at POI (Z_{th}), output variation of the DG, and voltage profile changes, which will be discussed in the next chapter, Z_{th} will also be included in the proposed network reconfiguration scheme. A summary of this relationship is presented below:

$$\Delta V_{POI} \propto Z_{th} \times \Delta P_{DG} \qquad (2.4)$$

The above equation will be considered in order to minimize the effect of intermittent and variable PV output on the voltage profile variations, and hence reducing the operation of voltage regulating devices in such situations.

The general outline of the proposed work is illustrated in Fig. 2.1.
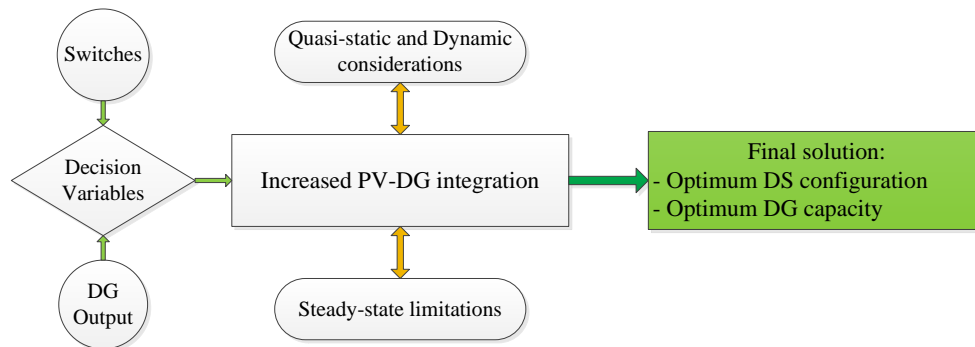
Figure 2.1: General outline of the proposed NR scheme

Valuable work have been performed on benefits of increased presence of DG, network reconfiguration in DS, and meshed topology, as discussed earlier. A brief big picture of the studied literature is provided here:

1. Static NR is proposed in [36–40,42] with different technical goals. The drawback of static NR is that another topology will be selected by the algorithm, if load profile changes. In [39, 40] where DG is also considered in the DS, DG profile is constant, and different output of the DG will also yield a different optimal solution selected by the proposed algorithms.

2. Dynamic NR is presented in [34,35,41,44,45]. However, the intermittent nature of variable renewable DG is not fully considered in these papers. Resolution of DG profile variation for [34,35,41,45] is hourly. An average load and PV value over a 4 hour period is used in [44], which has resulted in very smooth PV profile.

3. Number of switching operation might not be important in static NR; however, its importance is notable in dynamic schemes. In one test case performed based on the dynamic NR proposed in [35], 72 operations are seen daily. In [44] almost 30 operations are reported per day. Both papers have the optimization goal of minimizing the losses, but this number of switching operations poses a great burden on DS operators.

4. Less attention had been paid on NR for increasing hosting capacity of DS, until recently in [34]. The paper presents a NR scheme in planning framework, and the proposed method needs to be simulated for each time-step of the data beforehand. PV profile data resolution in this work is 1 hour.

In this work, network reconfiguration is used as a means to improve the hosting capacity of distribution systems to accommodate the increasing penetration levels of DG. More specifically, inspired from transmission and sub-transmission systems, DS meshed configuration is investigated and presented as a possible solution for increased renewable DG penetration. In summary, the following contributions are made:

- First, the work investigates the ability of DS meshed configuration to integrate more DG into the system. In this part of the work, the focus is on the steady-state operational characteristic of the system and the rated installed capacity of DG is considered. The following tests and contributions are performed:

    - A method is developed to estimate the maximum allowable DG power output in the distribution system.

    - Maximum allowable DG power output based on steady-state current and voltage limits are compared for different DG power factors, and for radial and different meshed configurations.

    - Selective meshed configuration is suggested as a solution for increased DG penetration.

- Second, a generalized formulation is required to select the optimum network configuration among possible radial and meshed topologies allowing for highest DG penetration. In this work, an optimization problem is hence formulated to consider steady-state voltage and current, with decision variables being the DG power output and the system topology. The following contributions are included:

    - An optimization problem is formulated as a generalized approach to have the highest allowable DG output in the DS.

    - The radiality constraint is relaxed in the network reconfiguration problem to allow for possible optimum meshed configurations.

    - Steady-state bus voltage and line current limits are considered as constraints.

    - Superior performance of selective meshed configuration is noted for both single and multi-DG scenarios.

- Finally, the intermittent and variable nature of renewable DG, especially that of PV-DG, is considered in the work, including:

    - The relationship between DG power variation and changes seen in the voltage profile is investigated.

    - Stiffness factor of DS at the POI, which is inversely proportional to the Thevenin impedance seen at POI, is found to be a governing factor in the above relationship.

    - DS meshed configuration can reduce the Thevenin impedance at the POI. This in turn can increase the stiffness factor. Therefore, DS meshed topology is investigated for possible reduction in voltage profile changes due to variable DG output.

– Then, the Thevenin impedance is incorporated in the network reconfigura-
tion problem and meshed configuration is used to not only allow for higher
DG power rated capacity, but also to reduce the voltage profile variations
while integrating renewable DG, which leads to improved operation of DS,
including less bus voltage variations and fewer voltage regulator tap oper-
ations.

This work hence pays attention to an important need for the industry, where pen-
etration of variable DG such as solar is limited by the negative impacts on voltage
profile due to the intermittent nature of such resources [87]. The proposed NR scheme
benefits from allowing meshed topology for DS, and knowing that meshed DS will
typically improve voltage profile and reduce power losses, these benefits are inherited
to the proposed NR scheme. Attention is paid to the relationship between voltage
variations seen in the feeder and the power fluctuations of an intermittent DG, and
by selecting the most robust topology, less voltage variations in presence of such re-
sources is expected. Due to the estimating technique presented, within a selected
time period, there would be no need to run the algorithm for each data point, and
hence, teh algorithm would be robust to load variations.

CHAPTER 3: SENSITIVITY-BASED APPROACH TO DETERMINE MAXIMUM INSTALLED DG CAPACITY

3.1   Overview

For both planning and operation purposes, it is important to know the maximum allowable limit that a DG can inject to the distribution system before operating limits are violated. In this chapter, the hosting capacity of DS is of interest considering a snapshot of DS while the steady-state voltage and current limits are considered. This means considering a known value for loads, and determining the maximum power output of the DG units in the system in that loading condition. Calculating this maximum value can be done using the repetitive power flow method [21]. This method considers a small power injection at the bus whose maximum allowable DG output is to be calculated. Then, it checks all voltage and current limits for violations. If no violation has occurred, the injected power is increased until a violation happens, and the final injection would determine the maximum allowable injection at the bus under study. Although accurate, this method requires repetition of power flow for each value of power injection, and hence requires a significant amount of time and computational burden.

In this chapter, an approach based on sensitivity analysis to determine the maximum allowable DG output is presented. The approach runs power flow in the system once, and using closed-form equations based on the Jacobian matrix of the Newton-Raphson power flow method [88], determines the maximum allowable DG output which does not violate any voltage or current limits. This method is then used to compare the hosting capacity of DS for alternative system topologies including both radial and meshed configurations, thus investigating the ability of meshed topology

to increase hosting capacity.

3.2   Repetitive Power Flow

The maximum allowable real power that a DG can inject into the distribution system, based on steady-state voltage and current limits, can be determined using repetitive power flow method [21], which is used in this paper to validate the accuracy of the presented sensitivity-based approach.

In the repetitive power flow approach, power injection at the POI is set to an initial value of zero. The active power injection is then increased by a certain value. This value defines the accuracy of the repetitive power flow method. The reactive power injection is also updated knowing the power factor of the DG (DG_{pf}). After running power flow, bus voltages and line currents are checked for violations of their allowable limits. This iterative procedure is continued until a single violation in either bus voltages or line currents has occurred. A flowchart describing the repetitive power flow method is presented in Figure 3.1. It is to be noted that since in the system without DG, all voltages and currents are in the desired limit, the iterative procedure is run at least for one iteration of increasing the injected power at the desired bus.

The repetitive power flow approach requires running power flow in each iteration. Power flow equations, by nature, are nonlinear equations relating voltage and power in the system. In order to solve this nonlinear set of equations, iterative solution methods are required, such as the Newton-Raphson method [88]. In distribution systems, where number of buses is large, running power flow has a high computational burden, and performing power flow calculations in each iteration until the final answer is achieved is time consuming as well. Thus, it is preferred to avoid the repetitive power flow method for determining maximum allowable power injection at a bus. Since this maximum allowable DG power output is calculated considering a snapshot of the DS, avoiding the use of repetitive power flow method enables the operator to update this maximum allowable value dynamically when changes such as loading
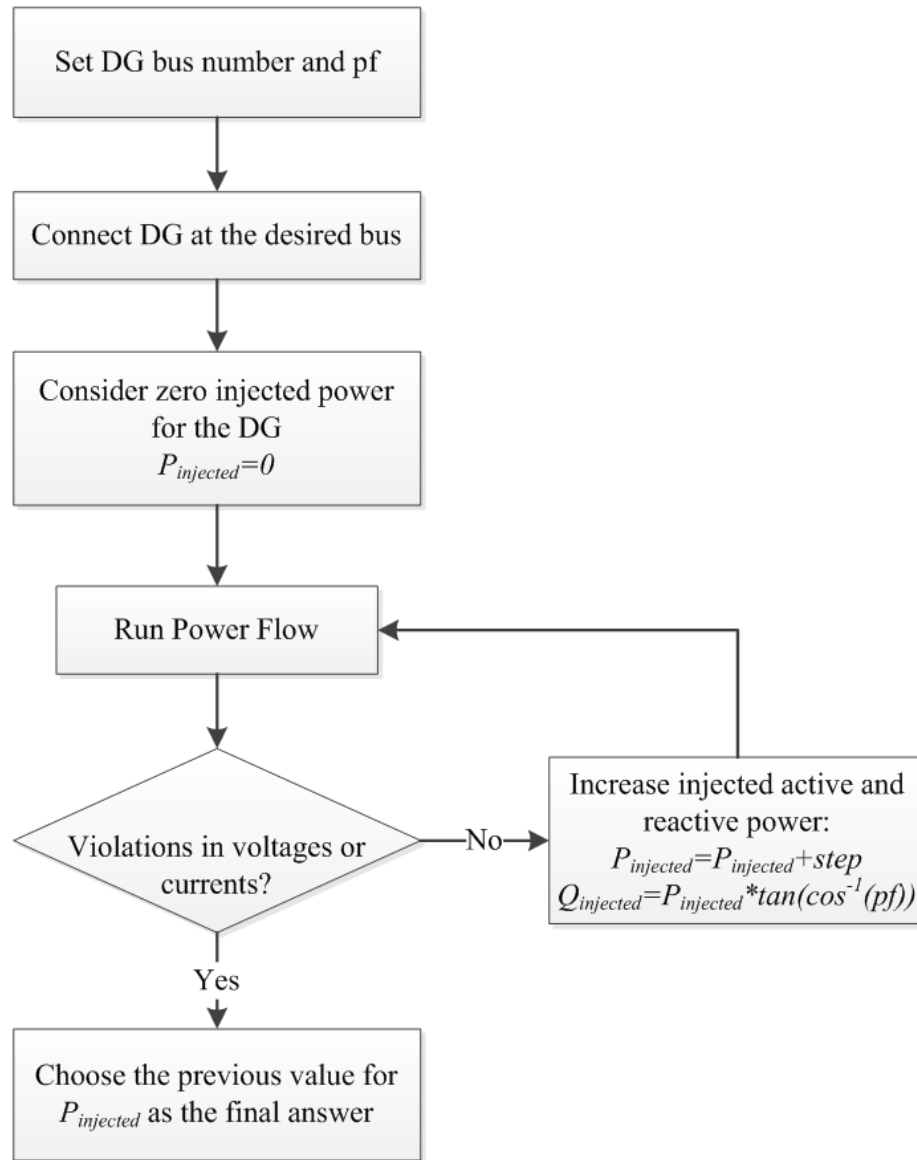
Figure 3.1: A generalized approach for the repetitive power flow method

conditions are observed in the system.

3.3   Sensitivity-Based Method

In the sensitivity-based approach, power flow is run once to determine the system voltages in the base case. By base case, it is meant the no-DG, no-change in DS topology scenario. A closed form equation is developed to relate changes between injected power from the DG and system voltages. Using this equation, the maximum

allowable DG injection considering voltage limits is achieved without requiring power flow iterations. Using the previous closed form equation, system voltages are updated in case of having the DG connected to the system and injecting the maximum allowable power based on voltage limits. Then, line currents are checked for violations of their limits. If any violation has occurred, the previous amount of DG injection is reduced until no violation occurs. In all these steps, there is no need to run power flow.

Knowing the power flow results of the base case, changes of voltage magnitudes and phases in case of adding a new source of generation, such as a DG, can be related to the active and reactive power injection of the new source by a linearization around the base case power flow results:

$$
\begin{bmatrix} \Delta P \\ \Delta Q \end{bmatrix} = \begin{bmatrix} J_1 & J_2 \\ J_3 & J_4 \end{bmatrix} \begin{bmatrix} \Delta \delta \\ \Delta V \end{bmatrix} \tag{3.1}
$$

where ΔP and ΔQ are vectors of changes in bus active and reactive power injections from the base case, and ΔV and $\Delta \delta$ are vectors of changes in bus voltage angles and magnitudes, respectively. The sub-matrices of the Jacobian matrix are defined as:

$$
J_1 = \frac{\partial P}{\partial \delta}, J_2 = \frac{\partial P}{\partial V}, J_3 = \frac{\partial Q}{\partial \delta}, J_4 = \frac{\partial Q}{\partial V} \tag{3.2}
$$

J_1, J_2, J_3 and J_4, will have dimensions $(n-1) \times (n-1)$, $(n-1) \times (n-1-m)$, $(n-1-m) \times (n-1)$ and $(n-1-m) \times (n-1-m)$, respectively, for an n bus system with m voltage-controlled buses [88]. It is to be noted that the substation is not considered in the above equations, since it acts as the system slack bus. Moreover, DGs are not usually participating in voltage control. Therefore, the aforementioned dimensions would be $(n-1) \times (n-1)$. Using (3.1), the following equations are

achieved:

$$\Delta P = \left(J_2 - J_1 \, J_3^{-1} \, J_4 \right) \Delta V = J_{RPV} \, \Delta V \tag{3.3}$$

$$\Delta Q = \left(J_4 - J_3 \, J_1^{-1} \, J_2 \right) \Delta V = J_{RQV} \, \Delta V \tag{3.4}$$

Hence, one can relate the changes in voltage magnitudes to variations in the injected active and reactive power in the system as:

$$\Delta V = V - V^0 = J_{RPV}^{-1} \Delta P + J_{RQV}^{-1} \Delta Q \tag{3.5}$$

where V^0 is the power flow result for the voltage magnitudes in the base case. Knowing the power factor of the investigated DG, ΔQ can be written in terms of ΔP. Therefore, the following equation can be written to evaluate the effect of injected active power by the DG connected at bus j, P_j, on the voltage at bus i, V_i, knowing the injected complex power has a power factor of pf_j:

$$\Delta V_i = V_i - V_i^0 = J_{VPQ_{ij}} P_j, \ i = 2 \ to \ N_{bus} \tag{3.6}$$

where:

$$J_{VPQ_{ij}} = J_{RPV_{ij}}^{-1} + J_{RQV_{ij}}^{-1} \tan(\cos^{-1}(pf_j)), \ i = 2 \ to \ N_{bus}, \ j = POI \tag{3.7}$$

The maximum allowable voltage variation of all buses can then be calculated from the power flow results for the base case. Assuming the maximum allowable change in voltage magnitude at bus i from the base case to be ΔV_i^{Max}, then the maximum allowable active power injection at bus j considering the voltage limit criterion for

bus i would be:

$$P_j^{Max,i} = \frac{\Delta V_i^{Max}}{J_{VPQ_{ij}}}, \; i = 2 \; to \; N_{bus} \tag{3.8}$$

Since all buses need to be considered, the minimum amount of all $P_j^{Max,i}$ values, for $i = 2$ to N_{bus}, would be the maximum allowable DG output at the Point of Interconnection (POI), i.e. bus j, considering voltage limits:

$$P_j^{Max,V} = \underset{i=2:N_{bus}}{Min} \{P_j^{Max,i}\} \tag{3.9}$$

After determining $P_j^{Max,V}$, the DG power output might need to be limited due to considerations such as maximum load that exists in the feeder, or due to the desired penetration level. Hence, the maximum allowable power injection at a certain bus considering such criteria as well as the bus voltage criteria is denoted by $P_j^{Max,V,DG}$.

Once $P_j^{Max,V,DG}$ is determined, the current limits are considered. Here as well, the use of power flow is avoided; currents are calculated based on a similar approach as mentioned above. First, knowing $P_j^{Max,V,DG}$, voltage magnitudes are updated based on (3.6); i.e., initial voltage is considered as V^0 (voltage in base case achieved from power flow solution), and then the injected power at bus j is set equal to $P_j^{Max,V,DG}$. Following a similar procedure, voltage phases can also be updated. With the updated voltage magnitudes and phases, line currents can be calculated. After calculating the currents, in case of line current violations, the value of $P_j^{Max,V,DG}$ is decreased in steps until line current criteria are satisfied. The final value of injected power would be the maximum allowable DG injection at the selected POI based on steady sate voltage and current limits, namely $P_j^{Max,Total}$. The procedure is summarized in the flow chart of in Fig. 3.2.
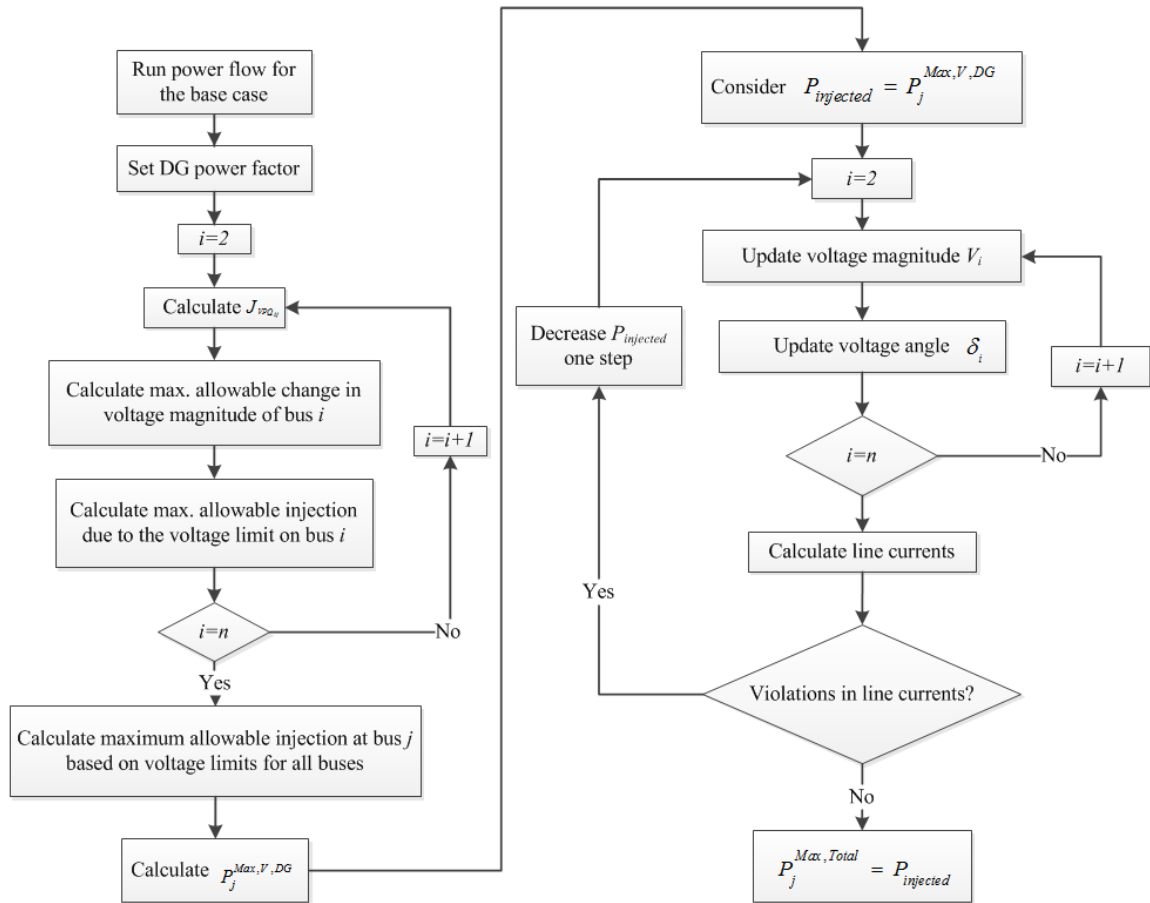
Figure 3.2: Sensitivity-based method to determine maximum allowable DG injection considering steady-state voltage and current limits

3.4 Assessment of Select Meshed Configurations: A Case Study

Using the described method, alternative meshed operation of distribution systems can be evaluated as potential long-term robust solution to increase maximum allowable DG penetration. In this section, results for the IEEE 69 bus system [89] are presented for radial and select meshed configurations. In this work, bus voltages are considered to be between 0.95 per unit (pu) and 1.05 *pu*, and currents have a maximum limit which might be different for the lines in the system. The obtained results verify the ability of meshed networks to accommodate higher DG penetration.

3.4.1 Test System: The IEEE 69 Bus Distribution System

The IEEE 69 bus distribution test system [89], which is a 12.66 kV feeder in PG&E utility, is shown in Fig. 3.3 and used as the test case in this work. This test case is widely used in NR literature [34–38, 40–42, 44]; and hence is used as the primary test case in this dissertation. Detailed information of the system such as line current limits and loads connected to each node are described in [89]. Total active and reactive power load of the system are 3.802 *MW* and 2.694 *MVAr*, respectively. The voltage at substation is set to 1.04 *pu* to maintain all voltages in the desired range of 0.95 *pu* and 1.05 *pu*. As shown in Fig. 3.3, the system has 5 Normally Open (NO) switches that could be closed to change the system topology, including forming meshes. As the total load of the system is 3.802 MW, the DG output power is indicatively limited to 4 MW. For simplicity, the meshed operating condition which is achieved by closing T_i is named C_i.

3.4.2 Effect of System Configuration: Radial vs. Meshed

In order to show the changes in maximum allowable DG power output due to network reconfiguration, Figure 3.4 shows the system voltages in the base radial and the meshed case C_2 when the DG is connected to bus 27 for different values of output power with unity power factor. As can be seen in this figure, the voltages are gradually

increased with an increase in DG output, and when the DG output power reaches a maximum value, voltage limits are violated. Therefore, $P_{27}^{Max,V}$ would be 0.958 MW for the base case, and 2.498 MW for configuration C_2. Since these values are less than the 4 MW limit, and there is no line current violation in both cases, $P_{27}^{Max,V,Total}$ would be equal to the mentioned values for the respective DS topology. These values are achieved using the repetitive power flow method.

If the sensitivity-based approach is used, $P_{27}^{Max,V,Total}$ would be calculated as 0.92 MW and 2.38 MW for the base case and configuration C_2 , respectively. This shows good accuracy of the proposed method with a 4.5% absolute error. In order to validate the accuracy of the presented sensitivity-based approach, this method is used to determine the maximum allowable DG output and the results are compared with the repetitive power flow method. Since using the repetitive power flow method to determine the maximum allowable DG output at one bus is very time consuming, a start point for its calculations is considered first. This start value is 95% of the value obtained by the the presented sensitivity-based method. In more details, the repetitive power-flow method starts from 95% of the respective value (same bus, same configuration) achieved from our method, and increases the DG output by 0.1% each time, runs power flow, and checks for any possible voltage and current violations. If any violations are seen, the previous DG injection is selected as the final answer. Even using a start point for the repetitive power flow method, calculating the maximum
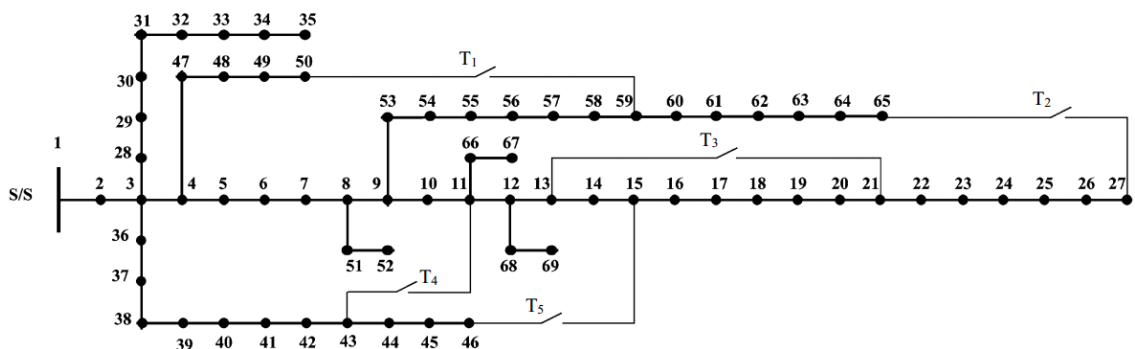
Figure 3.3: Test case system [89, 90]

a) radial
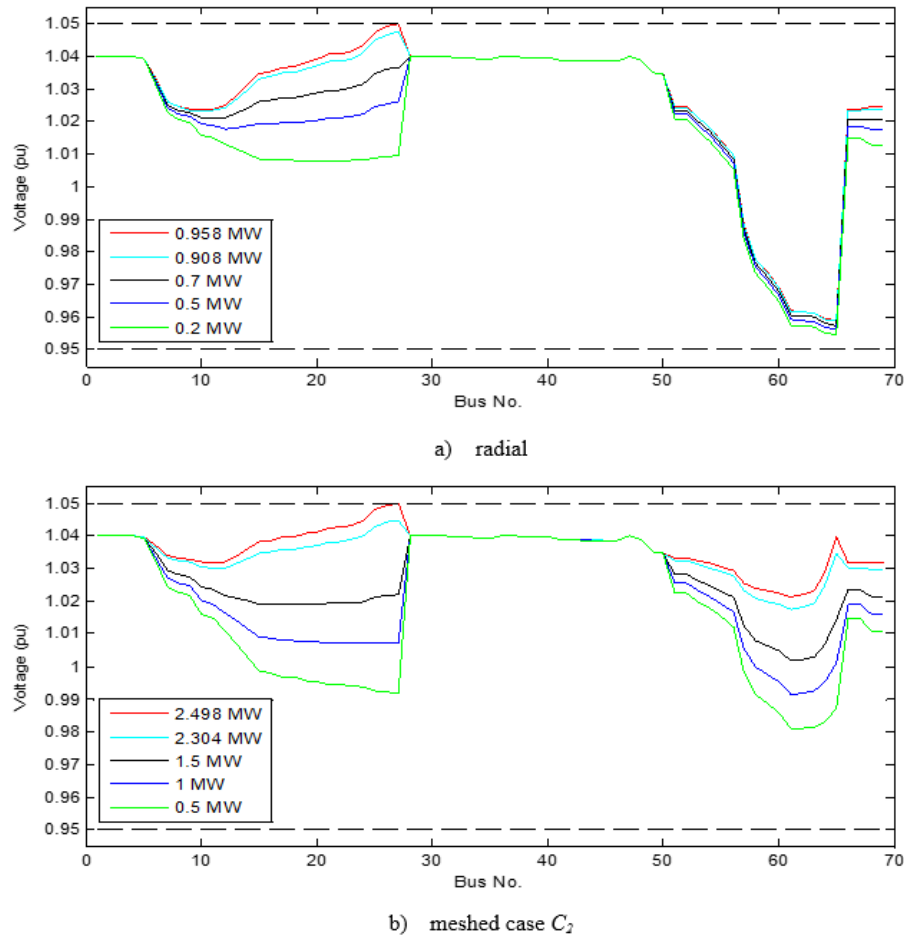
b) meshed case C_2

Figure 3.4: Bus voltages for different power injections at bus 27 in a) radial case and b) meshed case C_2

DG output at one bus in the system takes around 15 minutes on average, while the sensitivity-based approach provides the result in less than a second.

Table 3.1 shows the results of comparison between sensitivity-based method and the repetitive power flow method. Each column considers one topology of the DS, and presents the average and standard deviation value of error seen while estimating $P^{Max,V,Total}$ for differet buses in the test case using the sensitivity-based approach compared with the results of repetitive power flow method. As can be seen, the average error is around 4% in different cases, which shows good accuracy of the presented method.

Table 3.1: Error of calculating $P^{Max,V,Total}$ with the sensitivity-based method

	R	C_1	C_2	C_3	C_4	C_5
Average (%)	4.5	3.5	4.7	4.4	4.1	3.9
Std. Dev. (%)	2.4	1.4	2.3	2.4	2.2	2.2

In this section, the proposed sensitivity-based method for determining the maximum allowable DG power output is used to analyze the effect of meshed topologies. For this purpose, $P_j^{Max,V,Total}$ for all buses in the system (except the lack bus) are calculated separately for each configuration. Fig. 3.5 shows a comparison of each meshed configuration with the radial base case. Values of $P_j^{Max,V,Total}$ for base case are repeated in all plots in Fig. 3.5 for easier visualization.

As can be seen in Fig. 3.5, each meshed configuration has a different impact on maximum allowable DG power output at different buses in the system; i.e., it may increase this value at one bus while reducing it at another bus. It is hence noted that the configuration which allows the highest DG power output is not the same for all buses. Therefore, it is important to select the best possible configuration, given the desired POI bus, or select the best bus to install the DG in the specified configuration.
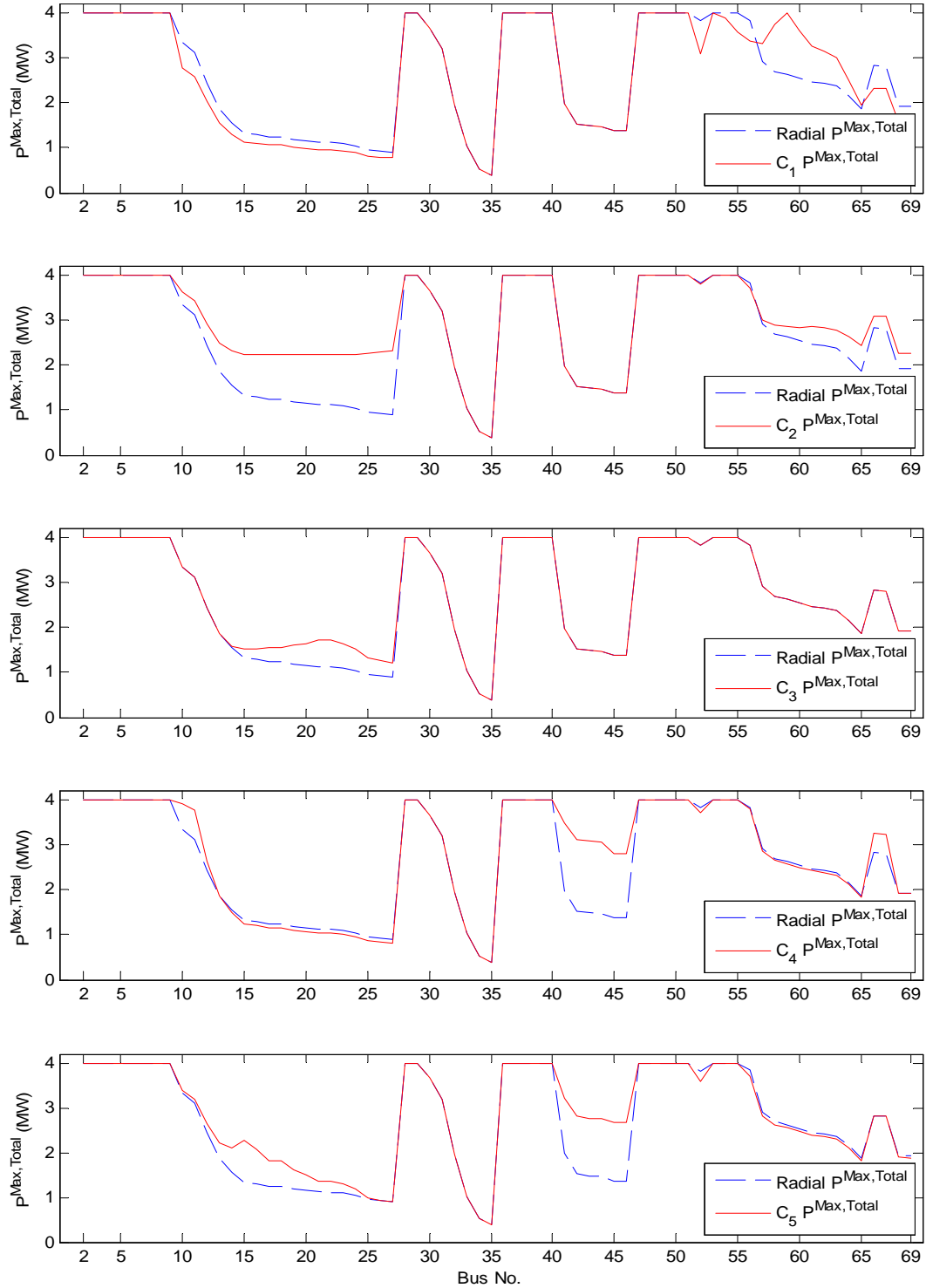
Figure 3.5: Maximum allowable DG injection for all system buses in different system configurations, DG unity power factor

3.4.3   Effect of Load Profile

Loads play an important role in determining the maximum allowable DG injection in the system. Voltage profile is typically higher in lower load values. Hence, system voltages are more prone to overvoltages in low loading conditions, and more limitations on the maximum allowable power injection in the system are expected. In order to study the impact of load profile on maximum allowable DG injection, loads are changed to 20% in the case study system. DG power factor is kept at unity, and values of $P_j^{Max,V,Total}$ for different configurations in minimum and maximum load profiles are shown in Fig. 3.6. As can be seen in this figure, as expected, for the same topology, the minimum demand scenario allows lower maximum power injection in comparison to the maximum demand scenario.
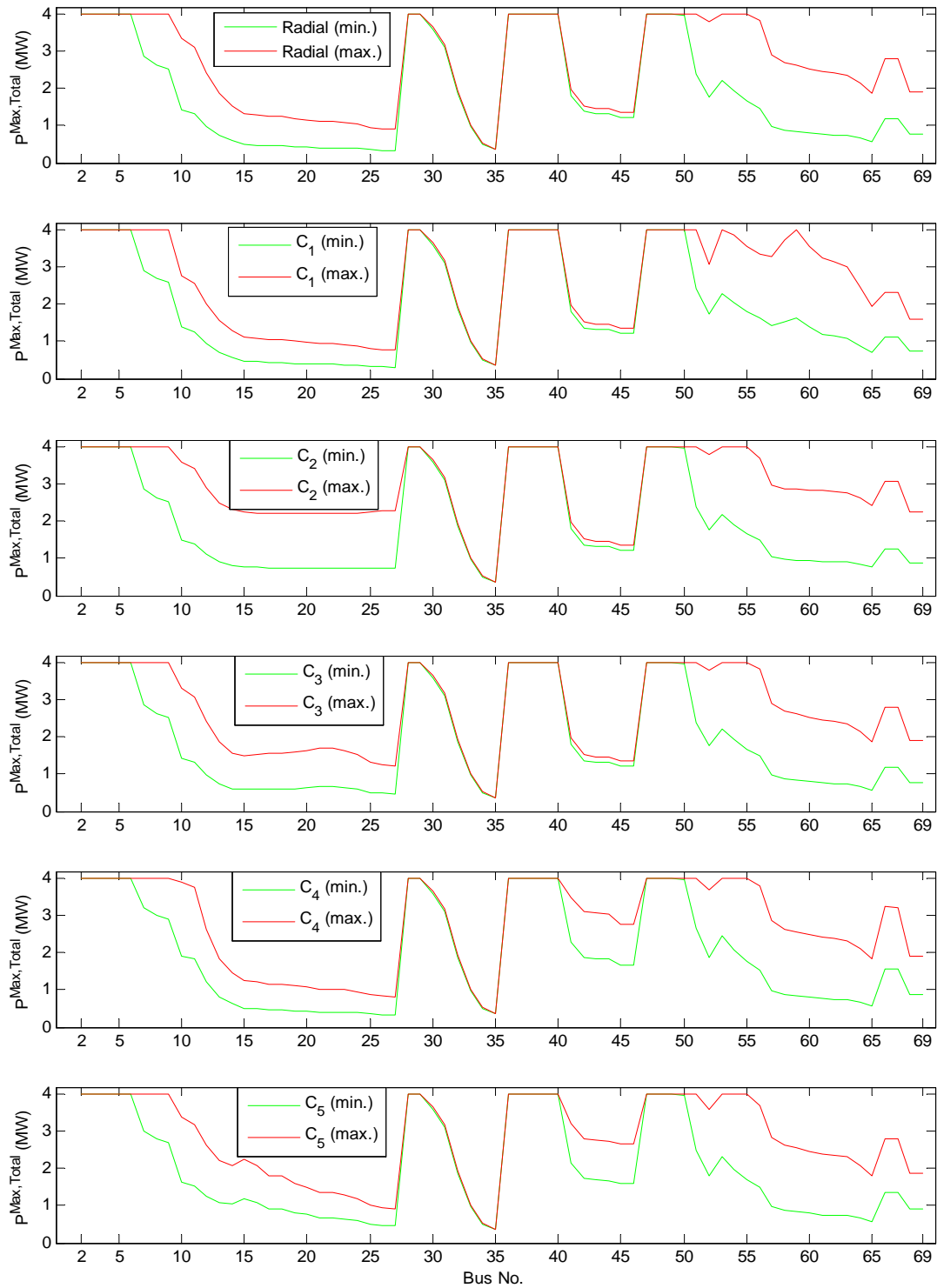
Figure 3.6: Comparison of maximum allowable DG injection in maximum and minimum loading conditions for different configurations

3.4.4   Effect of DG Power Factor

Impact of DG power factor can be studied as follows. The capacitive mode of operating the DG, i.e. generating reactive power from the DG, typically increases the voltages. Therefore, same values of injected active power in capacitive power factors will lead to higher changes in voltages in comparison to unity power factor mode. The maximum allowable penetration levels due to the voltage limits are expected to be lower than the unity power factor case, since the amount of maximum allowable voltage increase before reaching the upper limit would be reduced. A similar discussion is also valid for the general trend that the inductive mode of DG operation allows more power injection, since the DG absorbs reactive power and this absorption reduces the voltages. However, this might not always be the case: with increasing the absorbed reactive power, some voltages might violate the lower operating thresholds.

Figures 3.7 and 3.8 show the effect of system configuration on maximum allowable DG injection in different DG power factors. As Figure 3.7 demonstrates, although capacitive mode of DG operation decreases the maximum allowable DG power injection, meshed configurations allow more power injection in comparison with the radial configuration. A similar conclusion can be made for inductive power factors, as can be seen in Figure 3.8; i.e., meshed configuration can be used to increase the DG injection in comparison with the radial configuration for inductive power factors as well.

a) 0.9 capacitive power factor   b) 0.8 capacitive power factor
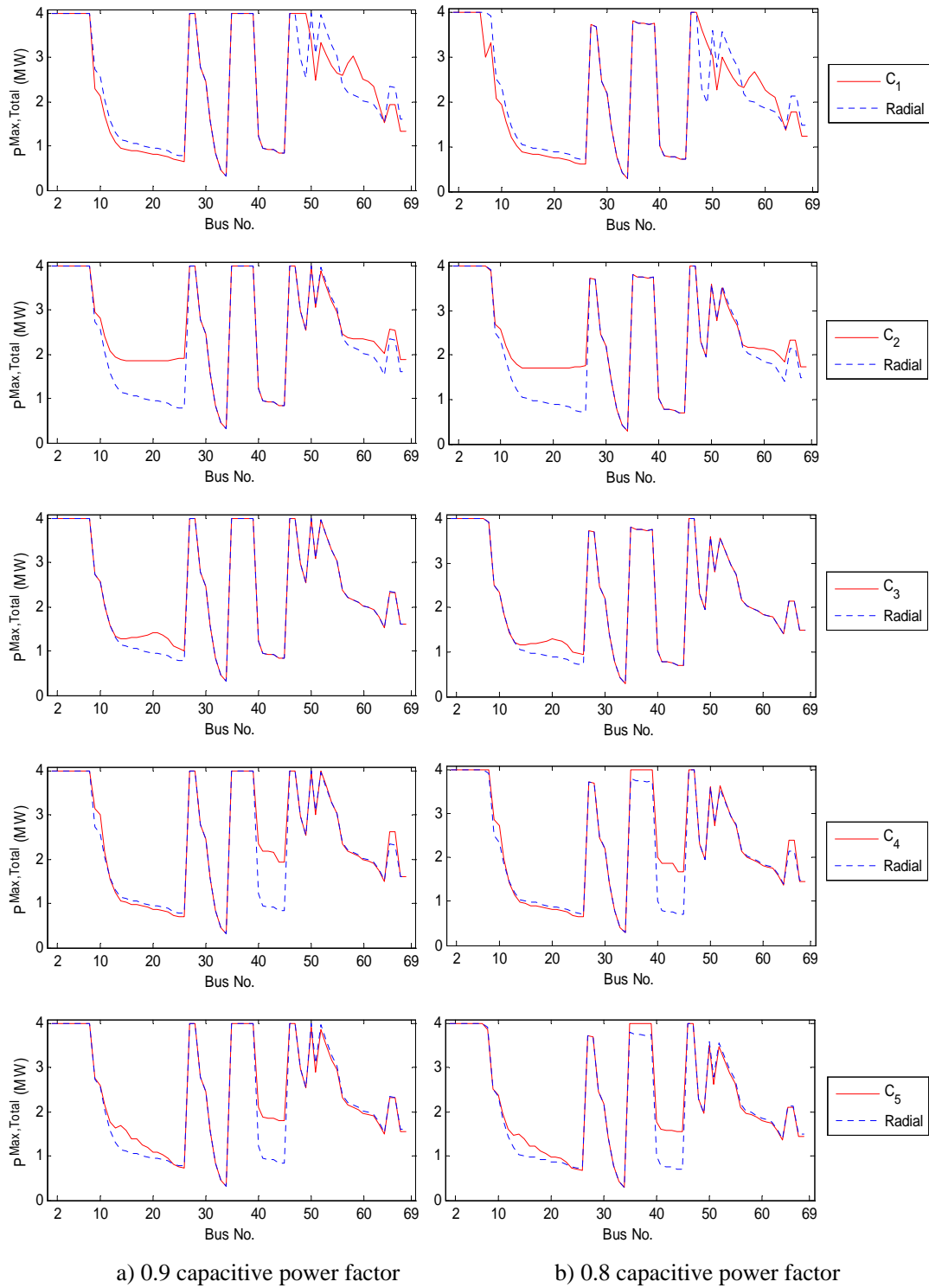
Figure 3.7: Maximum allowable active power penetration for different system configuration and capacitive mode of DG operation

a) 0.9 inductive power factor

b) 0.8 inductive power factor
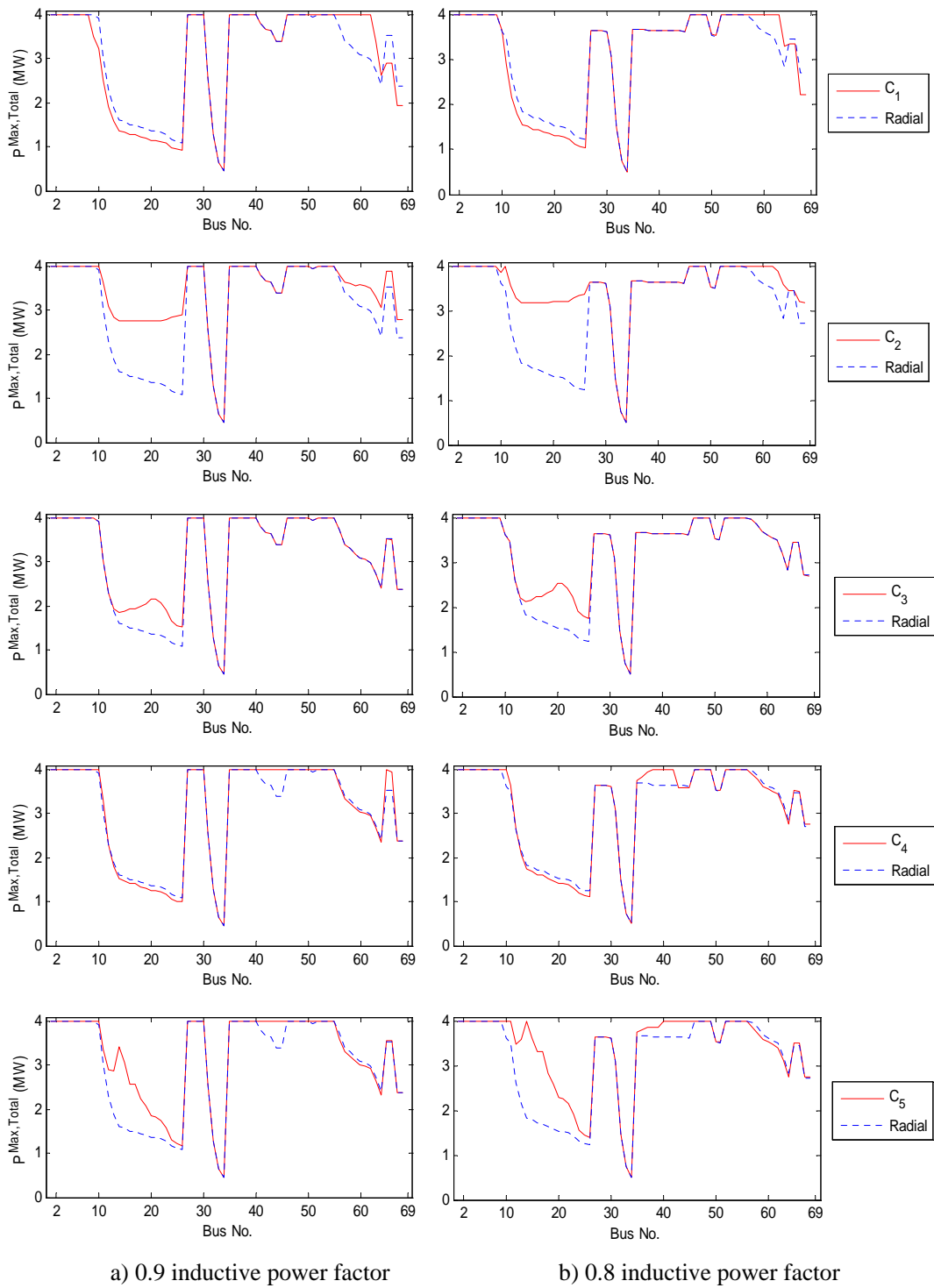
Figure 3.8: Maximum allowable active power penetration for different system configuration and inductive mode of DG operation

3.4.5   Summary of Results and Observations

In this chapter, a sensitivity based approach to calculate maximum allowable DG penetration was proposed, which considers steady state voltage and current limits. The proposed method is then used to compare the ability of radial and select meshed configurations for hosting higher DG penetration. The results have shown that, if chosen properly, meshed configurations can allow for higher levels of DG presence in the system.

Meshed configuration also generally results in lower power losses and improved voltage profile. As an example, power losses in the system for the maximum demand scenario with no DG for different configurations are shown in Table 3.2. As can be seen, active and reactive losses have been reduced moving toward the meshed topologies.

Table 3.2: Power losses in different DS topologies without DG installation

	Radial	C_1	C_2	C_3	C_4	C_5
$P_{loss}(kW)$	205.1	105.2	183.4	202.5	185.5	179.2
$Q_{loss}(MVAr)$	93.2	75	83.2	92.5	86	84.9

In the next chapter, a generalized network reconfiguration scheme is presented which determines the optimum topology to achieve the highest allowable DG power output in the system.

CHAPTER 4: INCREASING DS HOSTING CAPACITY THROUGH NR WITH RELAXED RADIALITY CONSTRAINT

4.1 Overview

This chapter proposes a method to increase distribution system hosting capacity by means of network reconfiguration. The presented approach is aimed at planning scenarios, and hence can be used when determining the rated capacity of DG installation such as PV is of interest.

Conventional formulations of the NR problem include the constraint to keep a radial topology. However, the radiality constraint is relaxed in the presented approach and both radial and meshed configurations are considered. To select the optimum configuration for increased penetration of DG, the method presents an optimization problem constrained by the steady-state bus voltages and line currents limits and then solves it with a proposed genetic algorithm. The presented method is then used to analyze the changes in hosting capacity of distribution system with respect to system topology in single and multi-DG scenarios. As results verify, distribution system meshed configuration can be seen as a possible approach to increase presence of distributed generation in the system, which also comes with side benefits of decreased real power losses and improved voltage profiles.

It is noted that introducing both meshed configuration and DG in the system needs careful attention, as they can help improve each others' benefits or might deteriorate each others' performance. This work aims at benefiting from both meshed configuration and presence of DG. By doing so, an effective distribution system meshed configuration can be selected as a robust solution for increasing the ability of distribution systems to withstand higher penetration levels of distributed generation.

4.2 Proposed Network Reconfiguration

The proposed NR problem formulation is aimed at increasing maximum installed DG capacity while maintaining system steady-state operating limits is also considered. Given the vector of states of switches in the system, S, the objective of maximizing total DG output is expressed by the objective function below:

$$\max_{S} \ G_P = \sum_{k=1}^{n_{DG}} P_{DG_k} \tag{4.1}$$

where P_{DG_k} is the active power output of the k th DG unit, and (n_{DG}) is the total number of DG installations in the system.

Steady-state bus voltages and line current limits should not be violated in the system. Considering N_{bus} as the total number of buses, and N_{line} as the total number of lines in the system, no voltage or current violation is permitted:

$$V^{min} < V_{bus_i} < V^{Max} \qquad\qquad for \ i = 1 \ to \ N_{bus} \tag{4.2}$$

$$I_{line_j} < I_{line_j}^{Max} \qquad\qquad for \ j = 1 \ to \ N_{line} \tag{4.3}$$

where i and j denote the i_{th} bus and j_{th} line in the system.

Moreover, only configurations that guarantee delivering power to all the loads are allowed in the reconfiguration procedure, i.e. no load should be dropped under the new system configuration. The set of all such configurations are selected using a graph-search algorithm, e.g. the Breadth First Search method [91], and denoted by S_U. Hence:

$$S \in S_U \tag{4.4}$$

As stated in the literature survey related to network reconfiguration schemes, the DS planner/operator might be interested in limiting the required switching operation

for achieving the optimal configuration. While enforcing a limit on the number of switching operation reduces the optimality of the main objective function, it is required to study its impact on the final results, and allows the DS planner/operator to select topologies with less optimal objective function value but reduced burden on the switches. The limitation on switching operation could be enforced by:

$$N_{SO} \leq N_{SO_{Max}} \tag{4.5}$$

where N_{SO} is the number of switch operations and $N_{SO_{Max}}$ is the maximum desired limit for this variable. Note that in this work, N_{SO} is calculated with respect to the base configuration.

In order to solve (4.1) with respect to the criteria mentioned above, an optimization problem is formulated in which minimizing the inverse value of (4.1) is considered, whilenew objective function is constructed in which minimizing thewhich considers the constraints as penalties and adds them to the inverse value of (4.1). This procedure is explained in the following text.

For each bus i, if its voltage violates the desired limits, cost of violation in voltage at bus i, namely C_{V_i}, is calculated as:

$$C_{V_i} = |V_i - V_{limit}| \tag{4.6}$$

where V_{limit} is the upper/lower voltage limit that bus i has violated, while both voltages in (4.6) are in per unit. If no violation has occurred in voltage at bus i, C_{V_i} would be zero. The same method would apply to the cost of violation in currents, C_{I_j}, considering whether current of line j, namely I_j, has violated its limit (I_{limit_j}):

$$C_{I_j} = \frac{|I_j - I_{limit_j}|}{I_{limit_j}} \tag{4.7}$$

Note that all system buses have the same higher and lower limits; however, each line might have its own limit in (4.7). Also, since the values of per unit voltages are typically around 1, the value of current violation for each line is divided by its limit so to give an equal weight to violations in voltages and currents. The same approach is used for (4.4) when $N_{SO} > N_{SO_{Max}}$:

$$C_{N_{SO}} = N_{SO} - N_{SO_{Max}} \tag{4.8}$$

and for (4.5) if $S \notin S_U$:

$$C_{load} = 1 \tag{4.9}$$

By incorporating the above constraints as penalties in the objective function, the following fitness function for the generalized NR scheme is defined:

$$\min_{S} \ F = \frac{1}{G_P} + \beta_S C_{N_{SO}} + C_{load} + \sum_{i=1}^{N_{bus}} C_{V_i} + \sum_{j=1}^{N_{line}} C_{I_j} \tag{4.10}$$

where different β_S can be set to 1 to consider the limit on switching operation, or zero to relax this criterion.

The optimization problem defined in this chapter is solved using Genetic Algorithm (GA), which is based on evolution theory [92]. Using GA enables the algorithm to solve the nonlinear equations (such as the load flow and the set of feasible configurations; i.e. S_U) involved in constructing the objective function. Overall, the following procedure is followed to solve (4.10) using GA. Initially, chromosomes are randomly created in a way that all of them guarantee delivering power to the loads, while the status of the switches is such that the "no-DG" scenarios do not violate any limits. Also, total DG capacity installed in the system is set randomly for each chromosome. Then, Newton-Raphson load flow is performed to calculate bus voltages and

line currents in the system while having DG generation and the network configuration indicated by each chromosome. Based on (4.10), the value of fitness function for each chromosome is calculated, and after sorting the individuals based on their corresponding fitness function values, pairs of parents are selected using the roulette wheel selection method [92], and single-point crossover is performed on them to generate two new children. Crossover rate is set to $Cross_{rate}$, which means that there is $1-Cross_{rate}\%$ chance that the parents are directly moved to the next step as children without any cross over. Note that the number of individuals in each generation is constant, therefore, steps 4 and 5 are repeated until enough chromosomes are created for the next step. After performing the crossover, specified percentage of the children are randomly selected for mutation to avoid the GA being trapped in local minima. After mutation, one iteration of the algorithm is completed. The above steps are then repeated until stopping criteria is met. The stopping criteria can either be chosen based on the percent of improvement in the best objective function value in two consecutive iterations of the GA, or can be set based on the number of generations produced by the GA. In this work, the stopping criteria is based on the total number of generations.

4.3   Case Study

The proposed methodology is used to select the highest amount of installed DG capacity without violations in the aforementioned constraints for different scenarios having single and multiple DG units. Then, a comparison is made between these maximum values with respect to the distribution system configuration. While focusing on the maximum allowable DG capacity, improvement in losses and voltages are also presented.

4.3.1   Test System and GA Parameters

The modified IEEE 69 node, 12.66 kV distribution system is used as shown in Fig. 4.1 [34–38, 40–42, 44]. Detailed information of the system such as line current limits and loads connected to each node is described in [90]. The total active and reactive power load of the system are 3.802 MW and 2.694 $MVAr$, respectively, and the voltage at substation is set to 1.04 per unit. Since the aim is to investigate both meshed and radial configurations other than the original topology of the system, NC switches S_6 to S_8 are considered to make other radial configurations feasible. The location and number of these switches are randomly selected for demonstration purposes. The problem consists of selecting the states of the switches to maximize the penetration level for the given/fixed location(s) of DG unit(s).
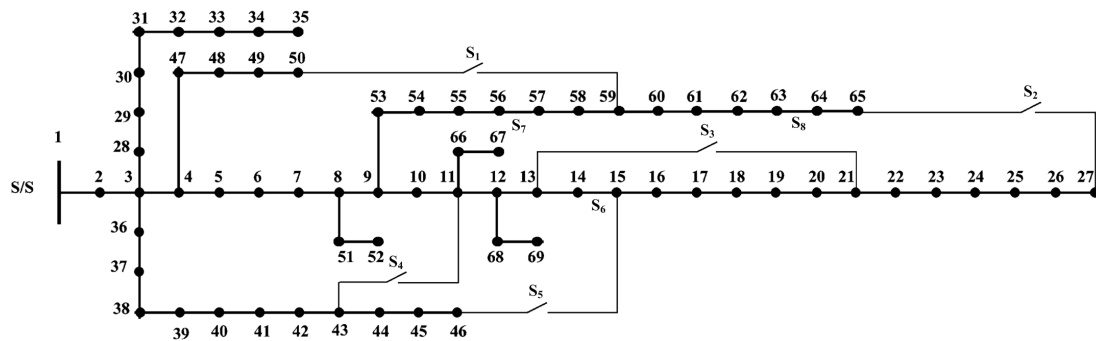
Figure 4.1: Modified IEEE 69 bus system [89, 90]

Due to the test system total load, each DG capacity is indicatively limited to 4 MW. For the specific test case, the total number of configurations that have no voltage and current violations in the no-DG scenario and energize all the loads is 130.

The first step in the GA solution method is to perform load flow for each chromosome to obtain bus voltages and line currents in the system. Knowing bus voltages, line currents, the P_{DG_k} value, and if needed, the value of $N_{SO_{Max}}$, the fitness function (4.10) value is calculated. Then, pairs of parents are selected using roulette wheel selection method [92] so that fitter chromosomes have the chance of being selected

as a parent more than once. Also, the best two chromosomes in each generation are directly moved to the next generation as elite members. For each pair of parents, single-point crossover is performed to generate two new children. 30% of the parents are then randomly selected for mutation to avoid the GA being trapped in local minima, while only 1 bit is mutated in each selected chromosome. Table (4.1) presents the required settings for the proposed GA in single-DG scenario. In this work, stopping criteria of 50 generations has shown promising results for single-DG scenarios, and it is increased by 10 generations per extra DG in the system.

Table 4.1: Settings for the proposed GA

Population Size	$Cross_{rate}$	Mutation rate	Stopping Criteria
100	80%	1.5%	50 Generations

Note that constraints introduced in (4.7), (4.6) and (4.9) are always imposed. Number of switch operations is discussed in each scenario separately.

4.3.2   Single-DG Scenario

In this part, a single DG unit is connected to the system and the best configuration for maximizing its injected power is achieved using the proposed optimization algorithm. The DG location is selected to be at the end of the laterals of the base case system (the original configuration). To show the effectiveness of the proposed method to allow for higher DG penetration, maximum allowable DG capacity at the selected points as POI, P_k^{Max}, is compared in two system configurations: 1. the base configuration and 2. the optimum configuration achieved by the presented method. Note that P_k^{Max} in the base configuration also considers steady-state voltage and current limits, but might not be equal to the value achieved from the optimum configuration. In order to calculate P_k^{Max} in the base configuration, repetitive power flow or sensitivity based method presented in Chapter 3 can be used.

The results of optimum P_k^{Max} values in the best configuration are compared with

the corresponding values in the base configuration in Table 4.2. In each row, a DG is connected at the selected POI and the proposed NR scheme is used to achieve the optimum DS topology. Hence, each row shows the maximum allowable DG capacities in the base configuration, status of switches for the optimal solution, maximum allowed capacity of the DG for the respective POI in the optimum solution, and the percentage increase in P_k^{Max} value moving from the base to the optimum configuration ($\Delta P_k^{Max}\%$).

Table 4.2: Optimum NR for select POIs, P_k^{Max} values and % increase in P_k^{Max} with respect to base configuration ($\Delta P_k^{Max}\%$)

| POI (k) | base conf. | Optimum Solution | | | | | | | | P_k^{Max} (MW) | $\Delta P_k^{Max}\%$ |
		S_1	S_2	S_3	S_4	S_5	S_6	S_7	S_8		
27	0.95	0	1	1	0	1	1	1	1	2.79	192
46	1.39	0	1	0	1	1	1	1	1	4.00	188
52	3.94	0	0	0	0	0	1	1	1	3.94	0
65	2.10	1	1	1	0	0	0	0	1	2.91	39
67	2.92	0	1	1	1	0	1	1	1	3.72	27
69	2.00	0	1	1	0	0	1	1	1	2.48	24

As seen in this table, changing the DS topology has the potential to increase the system maximum allowable DG capacity. Moreover, meshed configurations are shown to generally allow for higher DG capacities. With the exception of the POI at bus 52, where the base radial configuration is actually the resulting optimum configuration, meshed configurations result in higher allowable DG capacities. The results also reveal that for some buses, such as buses 27 and 46, $\Delta P\%$ is over 150%, which is a significant increase in the system hosting capacity. System hosting capacity when POI is bus 52 will be at its maximum in the base case, and the GA has also achieved this configuration as the optimum solution. This example shows that changing the configuration might not always help increase hosting capacity and needs to be done

selectively. System hosting capacity when the DG is located at bus 35 and when the DG is located at bus 50 are not changed with studied system configurations, and hence are not provided (P_{35}^{Max} is always 0.378 MW and P_{50}^{Max} is always 4 MW).

In order to validate the results of Table 4.2, the repetitive power flow method has been used to calculate maximum allowable DG capacity in all possible configurations;the best configuration with higher allowable DG is then selected. Since running the repetitive power flow method is time consuming, the sensitivity method presented in Chapter 3 (Fig. 3.2) is first used and then its final solution is fed to a repetitive power flow method which uses this initial data and then calculates the maximum allowable DG injection. The solution chosen by the presented NR algorithm matches the solution achieved by repetitive power flow method for all cases, however, note that using the same computer, the presented NR method takes less than a minute to obtain the results; while the repetitive power flow method combined with sensitivity method takes an average of 1.5 hours to find the optimum results.

As mentioned in Chapter 1, NR has been done in the literature to minimize losses or improve voltage profile in the system. Also, careful integration of DG in the system will help reduce losses and improve voltage profile. Therefore, although the presented NR in this paper focuses on increasing the hosting capacity of the system, it is interesting to look at power losses and voltage profile as side benefits of increasing hosting capacity through NR and potentially of using a meshed configuration.

A comparison of losses is shown in Fig. 4.2, which presents the total system active and reactive losses in three different scenarios which are normalized based on the respective losses in the base case ($P_{loss} = 205kW$ and $Q_{loss} = 93 \ kVAr$ in the base case). Note that base case here refers to the base configuration (no switch operation in Fig. 4.1) with no DG connected to the system. The three differnet scenarios for the results presented for each POI are 1) the base configuration having its maximum allowable DG power output at the respective POI, 2) the best configuration achieved

by presented NR without any DG installation, and 3) the optimum solution achieved by the presented NR method which includes the DG with the achieved highest possible power output. The second scenario is the case where no DG is installed in the system but the states of switches are selected as shown in Table 4.2 for each respective POI. This scenario is not the main focus of this discussion, as the state of switches is a part of the decision variable in the presented objective function and may not be investigated individually, but the results for this scenario have been presented to ease the comparison between the first and third scenario and to better analyze whether the change in the discussed attribute is due to the change in system configuration only or to the DG also. Results for buses 35 and 50 are not provided for the same reason as Table 4.2, and results for bus 52 are not provided as its optimum topology selected by the proposed NR scheme is the base configuration.

As this figure demonstrates, losses are significantly reduced with the optimum configuration, even more so than with the case of having P_k^{Max} injected into the base configuration. Specifically, Fig. 4.2 shows that:

- Installing DG in the base configuration at its maximum allowable level may decrease the losses.

- NR can also decrease the losses. Changing system configuration even without having the DG in the system has reduced losses more than the base case with DG at its maximum allowable level.

- The optimum solution achieved from the presented NR scheme, not only guarantees higher hosting capacity, it also significantly reduces losses.

This verifies the idea presented before which discusses that meshed configuration and DG injection can help boost each others' positive effects on the system.

As stated earlier in the introduction, reducing losses in the system yields an improved voltage profile. In order to study this effect, box-and-whisker plots are pre-

(a) $P_{loss}\%$

(b) $Q_{loss}\%$
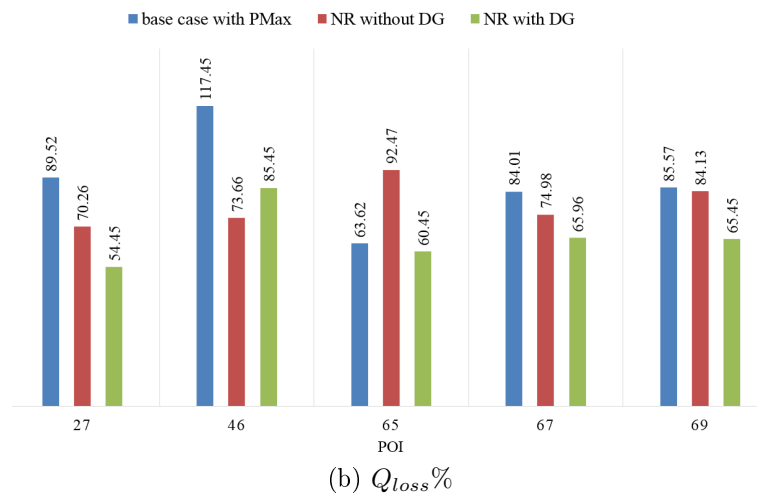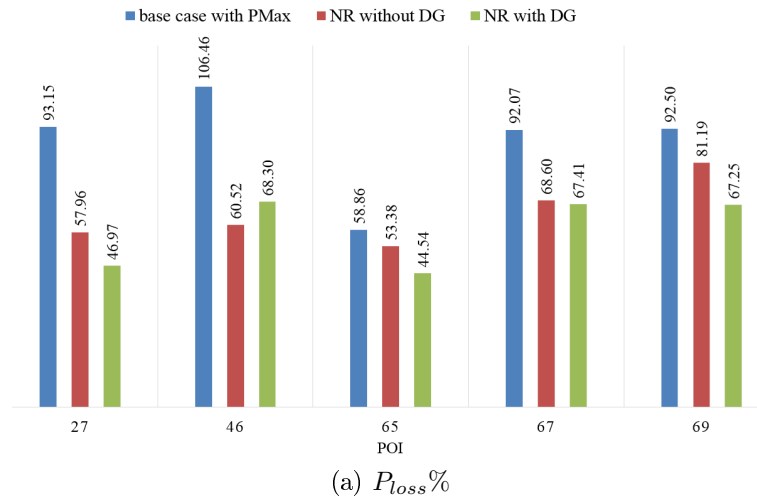
Figure 4.2: Comparison of a) active and b) reactive losses in three scenarios

sented in Fig. 4.3 for four different scenarios for two POIs. The four considered scenarios are: 1) base case, 2) base configuration with DG at its maximum allowable injection, 3) the configuration achieved from Table 4.2 for the corresponding POI without the DG, and 4) the best configuration achieved with the presented NR method receiving its maximum allowable DG injection at POI. Note that, like Fig. 4.2, the third case is presented here as an example of effect of changing the system configuration on voltage profile. The plots, drawn by MATLAB, are statistical plots that show the median (the central mark), 25th percentile (lower edge of the box), and 75th percentile (upper edge of the box). The whiskers extend to the minimum and

maximum data values. For better comparison, the average voltage for each scenario is also shown in its respective box and whisker plot with a star.
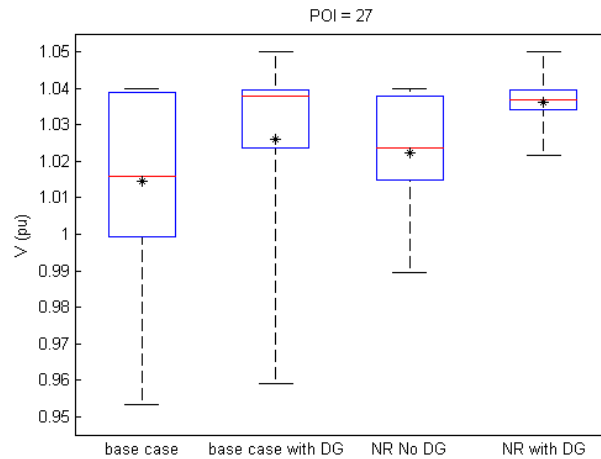
(a) POI = 27
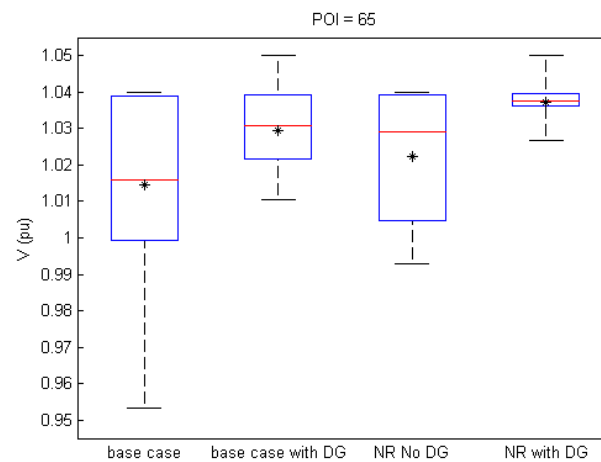
(b) POI = 65

Figure 4.3: Comparison of voltage profile in four scenarios for two POI

From Fig. 4.3, it can be seen that:

1. Keeping the system configuration unchanged, the DG injection at its maximum allowable limit has improved the voltage profile. Not only is the median and quartiles improved, the average voltage of the feeder is also improved. This is especially seen for Fig. 4.3b.

2. Changing the configuration alone has also improved the voltage profile. Not having another source in the system and also no capacitor installation has led

to having the same maximum voltage, but improved minimum, quartiles, and average value.

3. Applying the presented NR and injecting DG at its maximum allowable level has improved the voltage profile significantly. The voltage span (the difference between maximum and minimum), median, and quartiles are all improved. Therefore, although the proposed NR method does not consider voltage profile in its formulation, it not only guarantees more hosting capacity but also yields improvement in feeder bus voltages.

4.3.3   Multi-DG Scenario

In the single-DG scenario, the proposed NR method can select the best configuration with highest allowable DG injection without any violation accurately and in much less time than the repetitive power flow method. In a multi-DG scenario, the repetitive power flow method needs to search for all combinations of power dispatch from the DG units in each configuration, then selects the best configuration which allows for the highest total power injection into the system, i.e. achieving the highest hosting capacity. This time consuming and computationally burdensome procedure can be done with the presented NR scheme.

In order to have a better visualization of the possible improvement in hosting capacity with multiple DGs in the system, the maximum total DG injection in the distribution system is not limited, but each DG maximum capacity is limited to 4 MW. This is to study the effect of having two dispersed generation units each at a different location, and see if this results in an increase of the total DG injection compared to the case of a single DG. The results for two-DG scenarios are presented for select POI combinations as shown in Table 4.3.

As seen in this table, having DG at two different candidate buses has increased the distribution system hosting capacity in comparison with the single-DG scenario.

Table 4.3: NR results for 2-DG scenarios for select POIs

POI_1	POI_2	Optimum Switches								$P_{DG}^{Max}(MW)$			Losses		V_{span}^{pu}
		S_1	S_2	S_3	S_4	S_5	S_6	S_7	S_8	POI_1	POI_2	Total	kW	$kVAr$	
27	46	0	1	1	1	1	1	1	1	2.09	2.75	4.83	115.90	75.43	0.027
	52	0	1	1	1	1	1	1	1	2.25	2.54	4.79	107.24	56.24	0.026
	65	1	1	1	0	1	1	0	1	1.00	2.00	3.00	79.17	49.96	0.021
	67	0	1	1	1	1	1	1	1	2.06	2.39	4.45	104.76	55.77	0.027
	69	0	1	1	1	1	0	1	1	2.31	1.25	3.56	98.31	51.26	0.027
46	52	0	1	0	0	1	1	1	1	3.12	2.87	6.00	153.02	90.22	0.041
	65	1	1	1	1	1	1	0	1	2.50	2.44	4.94	101.12	72.80	0.023
	67	0	1	0	0	1	1	1	1	2.97	2.20	5.17	146.04	85.45	0.040
	69	0	1	0	0	1	0	1	1	3.34	1.25	4.59	145.78	92.35	0.047
52	65	1	1	1	1	1	0	1	1	2.37	2.44	4.81	90.03	50.97	0.019
	67	0	1	1	1	0	0	1	0	2.50	2.50	5.00	156.01	70.67	0.056
	69	0	1	0	1	0	1	1	1	2.94	1.58	4.51	157.24	68.00	0.051
65	67	0	1	0	1	1	1	1	1	2.24	2.33	4.58	101.56	54.74	0.019
	69	1	1	0	0	1	1	0	1	2.62	1.19	3.81	89.58	55.37	0.023
67	69	0	1	1	1	0	1	1	1	2.69	1.23	3.91	132.98	60.68	0.044

In all presented cases in Table 4.3, the total DG injection at the respective POIs is higher than the case where DG is located at either of the buses. For example, while P_{27}^{Max} and P_{46}^{Max} in single-DG scenario are 2.8^{MW} and 4^{MW}, respectively, the system can host a maximum of 4.8 MW when DG is divided between these two units.

4.3.4   Limiting the Number of Switch Operations

As shown in the previous sections, forming a meshed distribution system can increase its hosting capacity with respect to the radial configuration, which can lead to several benefits for the utility or system operator such as power losses reduction, improved voltage profile, etc. While the results provided in this work arethe hosting capacity of the DS in all possible configurations, it is interesting to see how the number of switching operations can affect the results. In order to do so, number of switching operations with respect to the base case, denoted by N_{SO}, is added to the optimization formulation, as mentioned earlier.

In order to compare the results of solving the optimization problem presented in (4.10) which also considers the limitation on N_{SO}, the values of P_k^{Max} for select POIs in 8 different conditions are calculated. In each condition, N_{SO} is set to a specific value, ranging from 0 to 7, where $N_{SO} = 0$ represents the base configuration. The results are seen in Table 4.4; where each row represents one POI. Each column represents a specific value of N_{SO}, i.e., the total configurations in which a total of N_{SO} switches have changed their status compared to the base radial configuration. The value of each cell represents the absolute percentage difference between the maximum DG capacity installed at the specified POI among all topologies with the given N_{SO}, and the maximum installed capacity at the same POI if no limit on N_{SO} is imposed. For instance, $POI = 27$ and $N_{SO} = 1$ shows the case of having DG only at bus 27, while N_{SO} is equal to 1. For each row, one specific value of N_{SO} yields the same P_k^{Max} as provided in Table 4.2, which is the global P_k^{Max} over all possible values of N_{SO} (with value of zero in Table 4.4). Value of other cells in each row are the absolute

percentage difference of P_k^{Max} for the respective N_{SO} in comparison with the global P_k^{Max}.

Table 4.4: Comparison of P_k^{Max} with respect to N_{SO}

POI	N_{SO}							
	0	1	2	3	4	5	6	7
27	65.70	10.57	3.34	0.00	0.02	0.66	0.96	1.48
46	66.76	31.57	12.51	0.00	1.23	4.13	13.25	16.39
65	28.15	4.46	9.01	3.76	0.37	0.00	0.48	0.81
67	21.34	10.42	2.66	0.00	0.12	3.85	8.21	19.55
69	19.25	4.97	0.00	0.24	1.16	5.95	14.52	19.41

For instance, for the case of having one DG unit at bus 27, $N_{SO} = 3$ yields the maximum possible P_k^{Max} among all N_{SO} values. Looking back at Table 4.2 reveals that this cell refers to $P_{27}^{Max} = 2.79\ MW$, which is results from the following system configuration $S = [0110111]$. For better explanation, consider limiting N_{SO} to 1 for the same case of $POI = 27$. By doing so, the maximum allowable DG injection at bus 27 would be achieved when N_{SO} is set to 1. This value is 10.57% less than the maximum allowable injection when N_{SO} is not limited in the presented NR scheme.

As can be seen in this table, P_k^{Max} has initially increased by changing the configuration, i.e. moving from $N_{SO} = 0$ (the base case configuration). However, there is an optimum point after which increasing N_{SO} further will decrease the P_k^{Max}. For example, in case of bus 27, the percentage difference of P_{27}^{Max} with respect to the global maximum is decreased from approximately 66% to 11% with 1 switch operation. By having 2 switch operations, the results improve significantly (only a 3.34% difference in DG capacity compared to the optimum configuration). For this POI, the best configuration occurs as a result of status change in 3 switches. The operator would then know that P_{27}^{Max} will only be improved by 3% with an extra switch operation, and might not be interested in this increment. It is also observed that, when POI is

bus 27, N_{SO} values of more than 3 will reduce the maximum hosting capacity of the DS.

CHAPTER 5: EFFECTS OF BUS IMPEDANCE MATRIX ON VOLTAGE VARIATIONS IN THE PRESENCE OF VARIABLE AND INTERMITTENT DG

5.1   Overview

Hosting capacity of distribution system was studied in the previous chapters, benefit of network reconfiguration was investigated, and meshed topology was shown to allow for higher DG capacity in DS. Different factors such as DG power factor and load profile were also discussed. Renewable distributed generation units introduce more challenges to the distribution system due to their variability and intermittent nature. While solutions such as employing battery energy storages can help produce smoother output profile for such DG units, it is required to provide a more robust solution by increasing the ability of DS itself for hosting higher capacities of variable distributed generation. This chapter pays specific attention to the impact of network topology on the way intermittent and variable DG output is mapped into the system voltages. Considering the equation governing this relation, a generalized NR scheme is provided which can reduce the impact of DG output variations on specific bus(es) of interest in the DS. Similar to the previous chapter, radiality constraint is relaxed to allow searching for both meshed and radial structures. The proposed NR scheme provides an optimum topology allowing for highest DG capacity with lowest bus voltage variations, which leads to benefits such as reduction of voltage regulator operations. Moreover, distribution system planners and operators can benefit from the provided perspective while the DG location is to be determined among select buses in the system.

5.2   Mapping the Variable DG Output to Changes in Bus Voltages

An important characteristic of the renewable DG units is that their output can change almost equal to its full capacity in a matter of few minutes [93]. For instance, Fig. 5.1 shows the output power of a real PV-DG in one month. These sudden and large changes are translated into voltage changes in the system, and can possibly cause voltage fluctuations. It is important to assess the impacts of such DG output variations on system voltages. The following two subsections provide the relationships between DG output variations and changes seen in bus voltages.
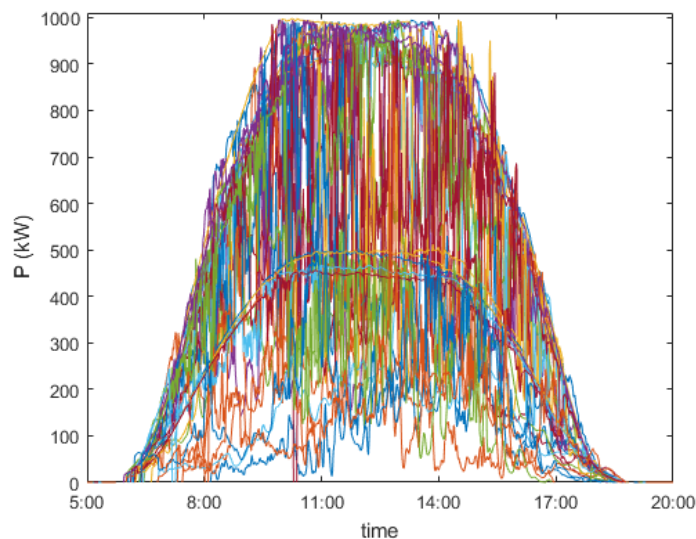
Figure 5.1: PV output profile of a 1 MW PV unit in one month, 1 minute data resolution

5.2.1   Considering Voltage Variations at the POI

Consider a distribution system with a DG which is modeled by a Thevenin equivalent circuit seen from the POI, depicted in Fig. 5.2. Y_{bus} of the simplified two-bus system can be formed converting the value of Z_{th} to admittance, namely y_{th}:
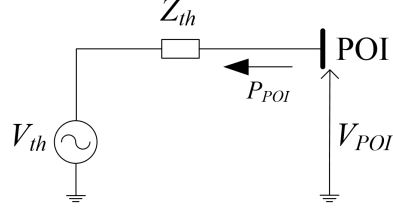
Figure 5.2: The Thevenin's equivalent circuit for the DS with DG connected at POI

$$Y_{bus} = \begin{bmatrix} y_{th} & -y_{th} \\ -y_{th} & y_{th} \end{bmatrix} \tag{5.1}$$

Let us define γ as (5.2) for brevity:

$$\gamma = \theta_{th} + \angle V_{POI} - \angle V_{th} \tag{5.2}$$

where $\theta_{th} = \angle Z_{th}$. In Chapter 3, the relationship between changes in active and reactive power injections with the vector of bus voltages were derived from Jacobian matrix of Newton-Raphson load flow, respectively, as repeated below:

$$\Delta P = (J_2 - J_1 J_3^{-1} J_4)\Delta|V| = J_{RPV}\Delta|V| \tag{5.3}$$

$$\Delta Q = (J_4 - J_3 J_1^{-1} J_2)\Delta|V| = J_{RQV}\Delta|V| \tag{5.4}$$

In Fig. 5.2, the Jacobian matrix is:

$$J = \begin{bmatrix} J_1 & J_2 \\ J_3 & J_4 \end{bmatrix} = \begin{bmatrix} \dfrac{\partial P_{POI}}{\partial \angle V_{POI}} & \dfrac{\partial P_{POI}}{\partial V_{POI}} \\ \dfrac{\partial Q_{POI}}{\partial \angle V_{POI}} & \dfrac{\partial Q_{POI}}{\partial V_{POI}} \end{bmatrix} \tag{5.5}$$

and since the following equations determine the power flow from POI to the system:

$$P_{POI} = -\frac{|V_{th}| |V_{POI}|}{|Z_{th}|} \cos\gamma + \frac{|V_{POI}|^2}{|Z_{th}|} \cos(\theta_{th}) \tag{5.6}$$

$$Q_{POI} = -\frac{|V_{th}| |V_{POI}|}{|Z_{th}|} \sin\gamma + \frac{|V_{POI}|^2}{|Z_{th}|} \sin(\theta_{th}) \tag{5.7}$$

J_{RPV} would be achieved as:

$$J_{RPV} = -\frac{|V_{th}|}{|Z_{th}|} [\cos\gamma + \sin\gamma \tan\gamma] + 2\frac{|V_{POI}|}{|Z_{th}|} [\cos\theta_{th} + \sin\theta_{th} tan\gamma] \tag{5.8}$$

In distribution systems, the voltage angle difference between buses is small [1], so considering $\angle V_{POI} \approx \angle V_{th}$ would yield:

$$J_{RPV} = \frac{2|V_{POI}| - |V_{th}|}{|Z_{th}| \sin\theta_{th}} = \frac{2|V_{POI}| - |V_{th}|}{R_{th}} \tag{5.9}$$

A similar procedure will lead to:

$$J_{RQV} = \frac{2|V_{POI}| - |V_{th}|}{X_{th}} \tag{5.10}$$

Therefore, the following equation relates Z_{th}, ΔP_{POI}, ΔQ_{POI}, and the voltage magnitude variation at the POI:

$$\Delta|V_{POI}| = \frac{R_{th}\Delta P_{POI} + X_{th}\Delta Q_{POI}}{2|V_{POI}| - |V_{th}|} \tag{5.11}$$

Considering voltage magnitudes to be close to the nominal value, the following is concluded from (5.11):

$$\Delta|V_{POI}| \propto R_{th}\Delta P_{POI} + X_{th}\Delta Q_{POI} \tag{5.12}$$

Defining the DG power factor as pf_{DG}, changes in V_{POI} per unit changes of active

power injected at POI would be related as follows:

$$\frac{\Delta|V_{POI}|}{\Delta P_{POI}} \propto R_{th} \pm X_{th}\tan(\cos^{-1}(pf_{DG})) \qquad (5.13)$$

As Q injection leads to a rise in the local bus voltage, (5.13) should be used with the positive sign for a capacitive pf_{DG}, and vice versa.

Equation (5.13) implies that, for example, in case of DG unity power factor at a POI and for an equal change in P_{POI}, the configuration with the lowest R_{th} will see the least voltage change at POI. This is in accordance with the terminology of stiffness factor [94], where stiffness is defined as the relative strength of the distribution system at POI compared with the DG, and is proportional to the short circuit current at the POI.

5.2.2   Bus Impedance Matrix (Z_{bus}) and Voltage Variations at a Remote Bus

Consider a distribution system with a renewable DG connected at POI. If the power flow results before experiencing changes in the DG output are known, one can write the following matrix equation when the DG output changes:

$$\Delta V_{bus} = Z_{bus}\Delta I_{bus} \qquad (5.14)$$

where V_{bus} is the bus voltage vector, Z_{bus} is the bus impedance matrix, and I_{bus} is the vector of injected currents. It is assumed that only the current at POI is changed, hence ΔI_{bus} would have only one non-zero array, i.e. ΔI_{POI}. Therefore, the following equation can be used to calculate the changes in the voltage at bus m:

$$\Delta V_m = Z_{POI,m}\Delta I_{POI} \qquad (5.15)$$

where $Z_{POI,m}$ is the element at the row representing the POI and the mth column of the Z_{bus}. Also, as:

$$I_{POI} = \frac{P_{POI} - jQ_{POI}}{(V_{POI})^*} \qquad (5.16)$$

where * denotes complex conjugate, one can rewrite (5.15) as:

$$\Delta V_m = \frac{(R_{POI,m} + jX_{POI,m})(\Delta P_{POI} - j\Delta Q_{POI})}{(V_{POI})^*} \qquad (5.17)$$

As assumed earlier, considering the imaginary part of voltages in DS to be negligible and $(V_{POI})^*$ to be 1^{pu}, (5.17) can be rewritten as:

$$\Delta |V_m| = R_{POI,m}\Delta P_{POI} + X_{POI,m}\Delta Q_{POI} \qquad (5.18)$$

Therefore, similar to (5.13), changes in V_m per unit changes of active power injected at POI would be related to:

$$\frac{\Delta |V_m|}{\Delta P_{POI}} \propto R_{POI,m} \pm X_{POI,m} \tan(\cos^{-1}(pf_{DG})) \qquad (5.19)$$

This equation is of great importance if bus m has a voltage-controlled capacitor, if a voltage regulator is set to control its voltage, or when it has an important voltage-sensitive load. In such cases, having the least possible variation in its voltage magnitude is of interest.

5.3   Proposed NR Scheme

Using the proposed equations in the previous section, a network reconfiguration scheme can be presented as a means for increasing the share of renewable DG in DS while diminishing negative impacts with special attention to bus voltage variations due to intermittent DG output. The proposed NR scheme can consider voltage at

POI or different bus of interest and present the DS topology in which the least impact
on desired bus voltages is observed.

As discussed before in Chapter 4, the NR scheme considers different criteria. For
better presentation, these criteria are repeated briefly here. (4.2) and (4.3) presented
the limits on steady-state bus voltages and line currents:

$$V^{min} < V_{bus_i} < V^{Max} \qquad\qquad for\ i = 1\ to\ N_{bus} \quad (5.20)$$

$$I_{line_j} < I_{line_j}^{Max} \qquad\qquad for\ j = 1\ to\ N_{line} \quad (5.21)$$

(4.4) was presented as the necessity of the configuration to deliver power to all the
loads:

$$S \in S_U \qquad\qquad (5.22)$$

In order to satisfy a minimum required DG penetration level, the following constraint
would also be considered:

$$P_{DG} \geq P_{desired} \qquad\qquad (5.23)$$

Finally, the limit on switching operation was introduced as (4.5):

$$N_{SO} \leq N_{SO_{Max}} \qquad\qquad (5.24)$$

In order to have the least impact from the variable DG output on the POI voltage,
as the discussion leading to (5.13) revealed, the following goal can be pursued:

$$\min_{S}\ G_{POI} = R_{th} \pm X_{th} \tan(\cos^{-1}(pf_{DG})) \qquad\qquad (5.25)$$

In the same manner, if there is an important voltage-sensitive node in the system,

such as a voltage regulator, one can consider the following goal to reduce the impact of the variable DG output on the voltage at a remote bus m:

$$\min_{S} \ G_m = R_{POI,m} \pm X_{POI,m} \tan(\cos^{-1}(pf_{DG})) \tag{5.26}$$

5.3.1 Increasing DS Hosting Capacity Considering Variations in Bus Voltages

If the installed capacity of DG unit is to be determined, or if it is dispatchable using an energy storage system, maximizing this installed capacity can be considered similar to the approach used in Chapter 4, (4.10). In this case, (5.26) and (5.25) can also be added to the previously mentioned formulation to consider the voltage variations due to DG output changes. In order to meet the minimum required penetration level of DG capacity, the following penalty factor for violating (5.23) when $P_{DG} < P_{desired}$ also added to the formulation:

$$C_{P_{DG}} = \frac{P_{desired} - P_{DG}}{P_{desired}} \tag{5.27}$$

where $C_{P_{DG}}$ is considered in per unit of the desired penetration level, in accordance with the discussion on (4.7).

Therefore, the following objective function is formed which can maximize the DG installed capacity, while mitigating the impact on bus voltage variations:

$$\min_{S} \ F = \frac{\alpha_P}{G_P} + \alpha_{POI}G_{POI} + \alpha_m G_m + \beta_P C_{P_{DG}} \tag{5.28}$$
$$+ \beta_S C_{N_{SO}} + C_{load} + \sum_{i=1}^{N_{bus}} C_{V_i} + \sum_{j=1}^{N_{line}} C_{I_j}$$

Variables α_P, α_{POI}, α_m are chosen by the operator to assign weight to each of the goals defined earlier. β_P can impose the minimum required installed capacity of DG units, and β_S can impose the criterion on maximum allowed switching operations.

5.3.2   Minimizing Variations in Bus Voltages with Given DG Capacity

Sometimes, the installed capacity of DG is already known. This may be due to previous calculations, limited availability of land, number of available solar panels and equipment, etc. However, there is still a need to perform a NR scheme in order to consider the variable and intermittent DG output and minimize its impact on bus voltages variations. Hence, in order to select the most robust DS topology based on the desired goals, the following scheme is presented:

1. Among all possible DS topologies, the ones which satisfy continuity of service to the loads (5.22) are selected. This is done thorough the graph-search technique discussed before [91].

2. The renewable DG output might be zero due to intermittency, clouding, or time of the day. Hence, select the topologies whose "no-DG" scenario satisfies voltage and current constraints, (5.20) and (5.21). If the load profile is variable in the time window under study, this can be done by selecting the maximum load profile. Then, with one iteration of power flow calculations, voltage and current limits can be checked for the topologies filtered by the previous step.

3. If $N_{SO_{Max}}$ is determined, select the topologies which satisfy (5.24). Otherwise, go to 4.

4. The selected topologies should be checked if they satisfy the desired DG output capacity. This can be done with one iteration of load flow, and checking the voltage (5.20) and current (5.21) constraints for all buses and lines. In this case, select the topologies that allow for the desired installed capacity at POI. For a variable load profile, day-time minimum load (when PV is expected to generate output) should be considered.

5. The following objective function can then be formed for each selected topology:

$$\min_{S} \; F = \alpha_{POI}G_{POI} + \alpha_m G_m \tag{5.29}$$

where α_{POI} and α_m can have different values to change the importance and weight of each desired goal in the system.

6. The topology with the least value of F is selected by the operator. The operator can also select the topology satisfying its maximum allowable switch operation.

5.4   Case Studies

In this section, the ability of proposed NR scheme for mitigating the negative impact of intermittent and variable DG on bus voltages is analyzed through presented simulation results. Similar to the previous Chapter, IEEE 69 node 12.66 kV test system as shown in Fig. 4.1 is used as test case. As a reminder, total load of the system is 3.802 MW and 2.694 $MVAr$, respectively; voltage at substation is set to 1.04 pu; and 3 NC and 5 NO switches are considered. Base case denotes the topology shown in Fig. 4.1 with no DG in the system, while base configuration refers to this topology while a DG might be connected to the system.

For the studies performed in this section, it is assumed that renewable DG is a PV unit. However, the presented method can consider data from any kind of renewable energy source. The active power output profile is selected as shown in Fig. 5.3, which is obtained from real data provided in [95], between 5:00 AM to 6:00 PM for April 24th 2016. For better presentation, the values are provided in per unit, and based on the maximum DG capacity required, the profile will be converted to MW.
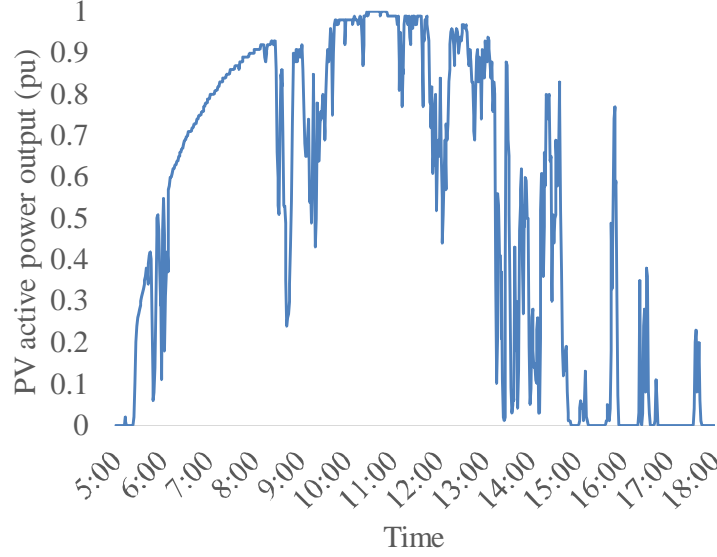
Figure 5.3: Sample DG output profile in per unit [95]

5.4.1   Scenario 1: Minimizing the Impacts on POI Voltage while Maximizing DG Penetration (G_{POI} & G_P)

In this scenario, minimizing the impact of DG output variation on POI voltage while maximizing its capacity to meet the desired penetration level is of interest. For this purpose, (5.28) is solved considering $\alpha_{POI} = 10$, $\alpha_P = 1$, and $\beta_P = 10$, while α_m and β_S are zero.

Solutions of the proposed approach for different buses of DG installation (POI) will lead to different values of DG capacity. Therefore, in order to enable the comparison between these different results, the following index is defined for changes seen in the voltage at bus i due to the variable DG profile with a maximum output value of P^{Max}:

$$V_i^{Ch} = \frac{\Sigma|V_i^{t_n} - V_i^{t_{n-1}}|}{P^{Max}} \qquad (5.30)$$

where n denotes the time instants in the study period.

In this study, value of $P_{desired}$ in (5.23) is selected equal to 1.9 MW to satisfy a minimum DG penetration of 50%, and a unity power factor is considered for the DG.

Solving (5.28) considering the values of the α and β parameters as mentioned above, the optimum states of switches, maximum allowable DG output, and the values of V_{POI}^{Ch} for each POI are presented in Table 5.1. As a reference, the value of V_{POI}^{Ch} and P^{Max} in base configuration are also presented. Note that the values of V_{POI}^{Ch} are in per unit voltage divided by 1 MW. As can be seen, the proposed NR scheme has minimized the value of G_{POI} in order to select a configuration in which the magnitude of V_{POI} will be least affected by the DG output variation; at the same time, the NR scheme has selected the maximum allowable DG generation in that configuration. The results show that the value of V_{POI}^{Ch} is significantly decreased in the optimum configuration.

Table 5.1: Best configurations for different POIs with a comparison of V_{POI}^{Ch}

POI	Optimum Solution			Base Configuration	
	S	P^{Max} (MW)	V_{POI}^{Ch}	P^{Max} (MW)	V_{POI}^{Ch}
27	11101111	2.626	0.444	0.958	1.750
46	11111111	3.624	0.201	1.391	0.269
65	11101111	2.762	0.463	2.089	1.498
67	11111111	3.189	0.242	2.922	0.415
69	11111111	2.068	0.416	2.006	0.658

As mentioned earlier, changing the power factor of DG can allow for increased DG penetration in the DS. For verification of the proposed methodology, effect of power factor is studied here. In general, capacitive power factors of DG will boost the voltages due to the injected reactive power, and the DG generating the same value of active power will lead to higher changes in voltages in comparison to unity power factor mode. One can conclude that, in general, the maximum allowable DG output is lower in capacitive power factors. This is also the reason for recommending inductive power factor operations of DG to the industry [96]. Similar conclusion can

be made for inductive mode of DG operation.

In order to study the impact of DG power factor, bus 27 is considered as POI among different simulations performed here. Therefore, a DG is connected to bus 27 with the output profile shown in Fig. 5.3. The value of $P_{desired}$ in (5.23) is selected equal to 1.9 MW. In separate utilizations of the proposed NR scheme, two different values of DG_{pf}, namely 0.9 capacitive and 0.9 inductive, are considered. Moreover, in order to see the impact of number of switch operations, 8 values of N_{SO} are considered separately. The optimum states of switches, maximum allowable DG output, and the values of V_{27}^{Ch} are achieved using the NR scheme presented in (5.28) with aforementioned coefficients ($\alpha_{POI} = 10$, $\alpha_P = 1$, $\beta_P = 10$, $\alpha_m = 0$), while β_S is changed to 100 to impose the desired maximum number of switching operations. The results are presented in Table 5.2.

Table 5.2: Impact of DG power factor on results of Scenario 1, POI= 27

| DG_{pf} | Optimum Solution | | | |
	N_{SO}	S	P_{27}^{Max} (MW)	V_{27}^{Ch}
	0	00000111	0.810	2.061
	1	01000111	2.063	1.160
	2	01001111	2.087	0.789
	3	11001111	1.930	0.650
$Cap.$ 0.9	4	11101111	2.089	0.558
	5	11111111	2.085	0.559
	6	11111011	2.084	0.561
	7	11111001	2.183	0.584
	0	00000111	1.187	1.411
	1	01000111	3.279	0.730
	2	11000111	3.493	0.471
	3	11001111	3.323	0.377
$Ind.$ 0.9	4	11101111	3.611	0.323
	5	11111111	3.616	0.322
	6	11111011	3.572	0.327
	7	11111001	3.813	0.334

Compared to the base configuration, improvements achieved by the NR scheme are visualized by comparing both the values of P^{Max} and V_{27}^{Ch} for capacitive as well as

inductive cases. As can be seen in this table, allowing the NR scheme to change the topology of DS with any given permitted of N_{SO} has led to an increased allowable DG capacity while reducing the changes seen in the POI voltage during the simulation period (780 minutes). For the capacitive and inductive case, N_{SO} equal to 4 and 5, respectively, have led to the lowest V_{27}^{Ch} value. The operator can also select the desired network topology based on the limitation on switch operations. As expected, the values of V_{27}^{Ch} for inductive power factors are less than the capacitive cases of operating the DG, while in the same time, higher DG capacity is allowed in the inductive operation modes.

5.4.2 Scenario 2: Minimizing the Impacts on Remote Bus Voltage while Maximizing DG Penetration (G_m & G_P)

In this scenario, minimizing the impact of DG output variation on a remote bus of interest while maximizing its capacity and meeting the desired penetration level is of interest. For this purpose, (5.28) is solved considering $\alpha_m = 10$, $\alpha_P = 1$, and $\beta_P = 10$, while α_{POI} and β_S are zero.

Like before, $P_{desired}$ is set to 1.9 MW with a unity power factor and (5.28) is solved considering the values of the α and β parameters as mentioned above. The NR scheme finds a configuration with minimum value of 5.26 while allowing for higher DG installed capacity. In order to analyze the effect of DG output variations on a remote bus, bus m in (5.26) is considered to be bus 12 in this case. In Table 5.3, the results of proposed NR scheme in this scenario are presented. In each row, a different POI is selected and the respective optimum DS configuration is presented. Moreover, the maximum allowable DG output at the POI and value of V_{12}^{Ch} are compared in the optimum and base configuration, demonstrating that the value of V_{12}^{Ch} is significantly decreased in the optimum configuration, while higher DG capacity is permitted.

Table 5.3: Results of NR scheme in scenario 2 for different POIs

POI	Optimum Solution			Base Configuration	
	S	P^{Max} (MW)	V_{12}^{Ch}	P^{Max} (MW)	V_{12}^{Ch}
27	11001001	2.529	0.000	0.958	0.518
46	00001011	2.022	0.000	1.391	0.000
65	10111101	2.218	0.000	2.089	0.189
67	11111111	3.189	0.179	2.922	0.377
69	11111111	2.068	0.272	2.006	0.515

5.4.3 Scenario 3: Minimizing Variations in POI Voltage with Given DG Capacity

If the DG Capacity is already determined in the planning scenario, the steps mentioned in Section 5.3.2 can be followed to determine the best topology in order to have the least impact on POI voltage, setting $\alpha_{POI} = 10$ and $\alpha_m = 0$ in Step 5. For this purpose, POI is selected to be bus 27, and the DG power factor is considered unity at first.

First, all possible DS topologies which satisfy continuity of the service to the loads and also their no-DG case meets all voltage and current limits are selected. This is irrespective of the POI and since it does not consider the DG in selecting the pool of feasible configurations, it is independent of the DG power factor too. In the studied test case, 130 configurations meet both criteria of Steps 1 and 2 in Section 5.3.2, as mentioned above. Then, the topologies which allow for the desired maximum DG output (capacity) considering the desired DG_{pf} are selected. A total of 46 configurations allow for a DG installed at bus 27 with maximum capacity of 1.9 MW, and unity DG power factor. Finally, the configuration with the least value of (5.25) and hence least value of (5.29) is selected. This will yield the status of switches as [1 1 1 0 1 1 1 1].

In order to visualize the result mentioned above, load flow has been performed

for all 46 configurations which allow for the desired penetration level, do not drop the load, and their no-DG scenario meets the requirement for bus voltages and line currents. Load flow is performed for 780 minutes during the study period (5:00 AM to 6:00 PM). Note that the DG output profile is equal in all 46 configurations to enable the comparison between voltages in the plot. Voltage at bus 27 (POI) is statistically analyzed using the box and whisker plots shown in Fig. 5.4. The x-axis of the plot shows the values calculated for (5.25), which are sorted in ascending order. The boxes show the first quartile (lower edge of the box), median (the central mark) and third quartile (upper edge of the box) of V_{27} for the respective configuration, while the whiskers extend to the minimum and maximum values. For better comparison, the average voltage for each configuration is also shown in its respective box and whisker plot with a star.
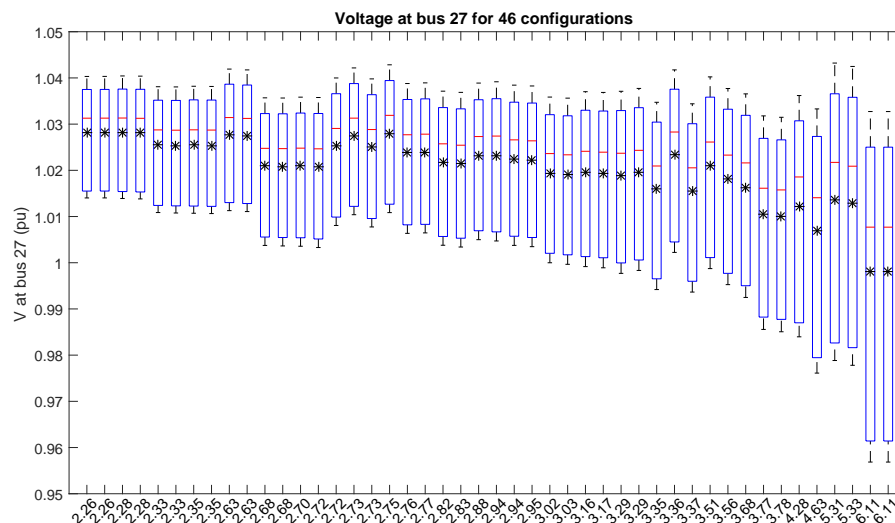

Figure 5.4: Box and Whisker plots for V_{POI} (POI=bus 27) for 46 configurations, unity power factor

As can be seen in this figure, the configurations with lower values of (5.25) have led to less variation in the voltage magnitude changes at POI. It is worth mentioning that, although the relationship provided in (5.13) was calculated to approximately estimate the voltage changes in POI, the accurate results calculated with load flow

match this equation. The same results are provided in Fig. 5.5. This figure shows the voltage at bus 27 for all 780 minutes of the simulation in 46 different configurations. As can be seen in this figure, voltage of this bus has had less variations in topologies with smaller values of (5.25).
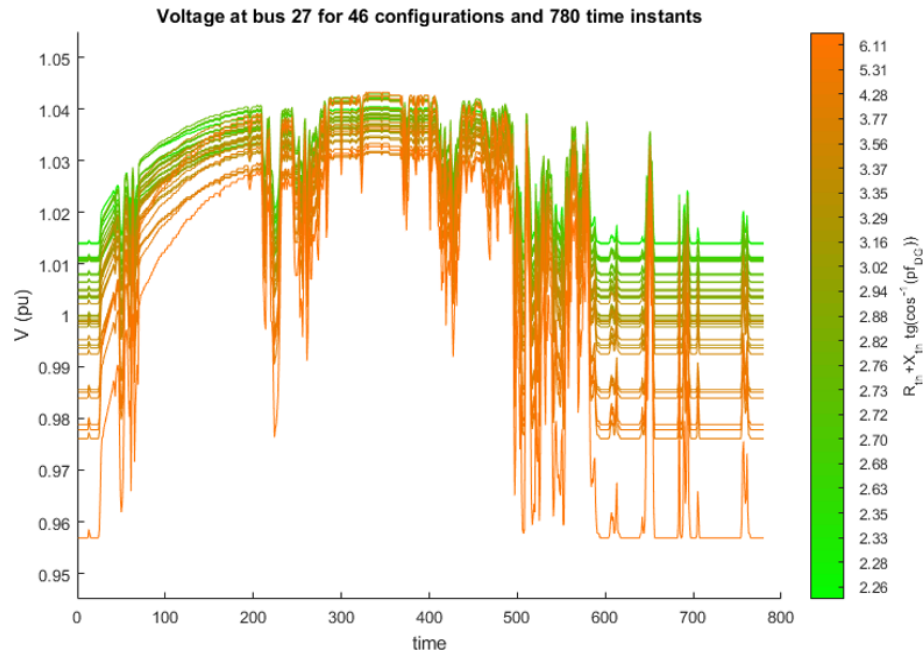

Figure 5.5: Heat plot for V_{POI} (POI=bus 27) for 46 configurations

If the changes seen in voltage at bus 27 between each consequent snapshots are of interest, values of (5.30) can be studied, especially since the value of P^{Max} is equal in the simulations for all 46 configurations.

In order to study the impact of DG power factor, two cases are considered and similar methodology has been used to select the optimum configuration for least changes seen in voltage at bus 27. Among the total 130 configurations which do not drop the load and have acceptable no-DG conditions, a total of 39 configurations allow a DG with 0.9 capacitive power factor and 1.9 MW maximum capacity. Then, the topology with the least value of (5.25) is selected by the proposed NR scheme, which denotes the status of switches as [1 1 1 0 1 1 1 1], which is similar to the unity power factor case; i.e., the configuration among the 46 candidates which had the least
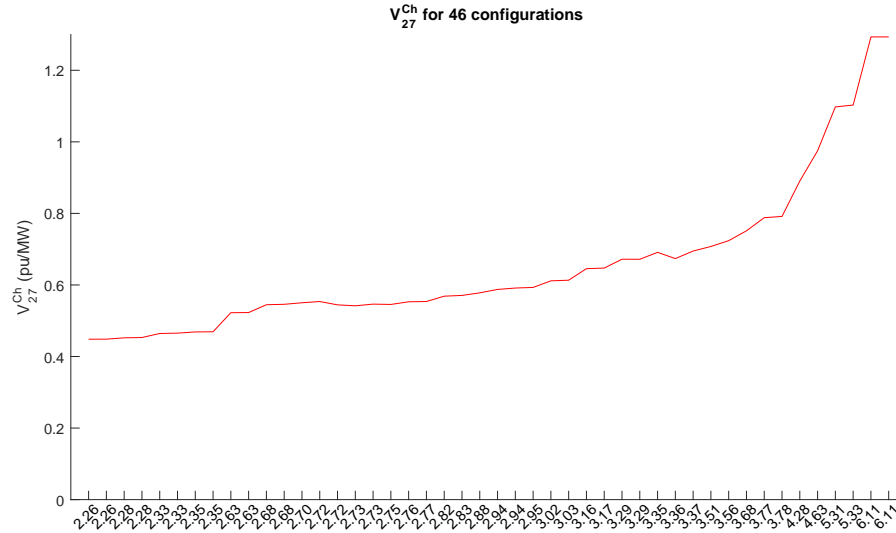
Figure 5.6: Comparing voltage changes at V_{POI} (POI=bus 27) for 46 configurations using V_{27}^{Ch}, unity DG power factor

R_{th} value is selected among the 39 candidates for capacitive power factor since it has the least value of $R_{th} + X_{th} \tan(\cos^{-1}(0.9))$. Box and whisker plots for voltage at bus 27 for the duration of study in all 39 configurations are shown in Fig. 5.7, which are sorted based on the value of (5.25) for the topology they introduce. As can be seen in Fig. 5.7, voltages are generally higher than the unity power factor of DG as expected. This intuitively verifies previous findings that maximum allowable DG injection in capacitive mode of DG operation is expected to be less than the unity power factor. Moreover, as can be seen in Fig. 5.8, the minimum achieved value of changes in the voltage at bus 27 is higher than the case for unity DG power factor.

Based on above statements, similar observations can be expected for 0.9 inductive power factor of DG. In this case, a total of 56 configurations allow for the desired penetration, which is more than the other two cases with unity and capacitive power factors. Fig. 5.9 shows that the same trend is observed among different configurations, i.e. topologies with smaller values of (5.25) have led to smaller changes in voltage of POI. The optimum configuration selected by the NR scheme is achieved when all NO switches are closed. The second best configuration is similar to the previous two
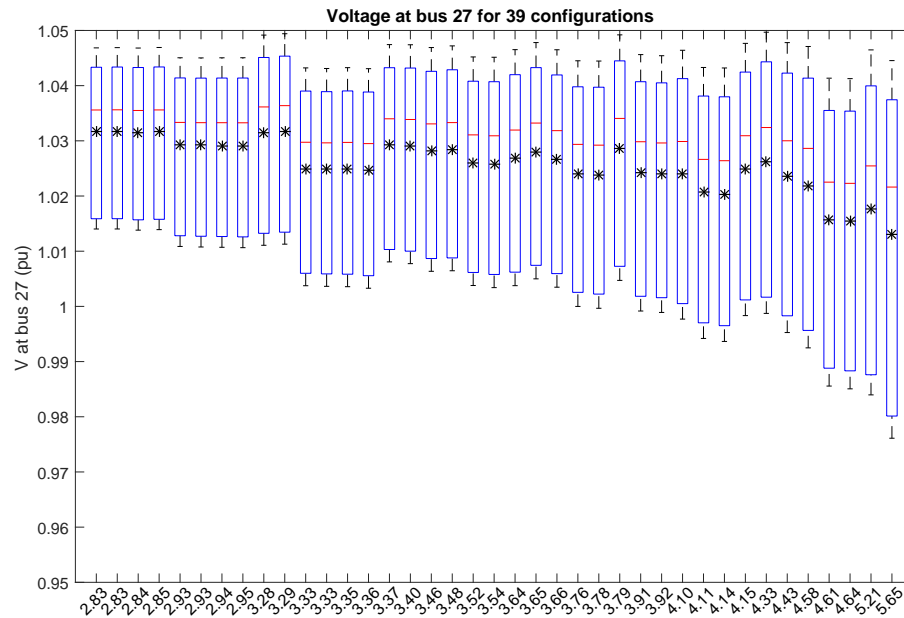
Figure 5.7: Box and Whisker plots for V_{POI} (POI=bus 27) for 39 configurations, 0.9 capacitive power factor
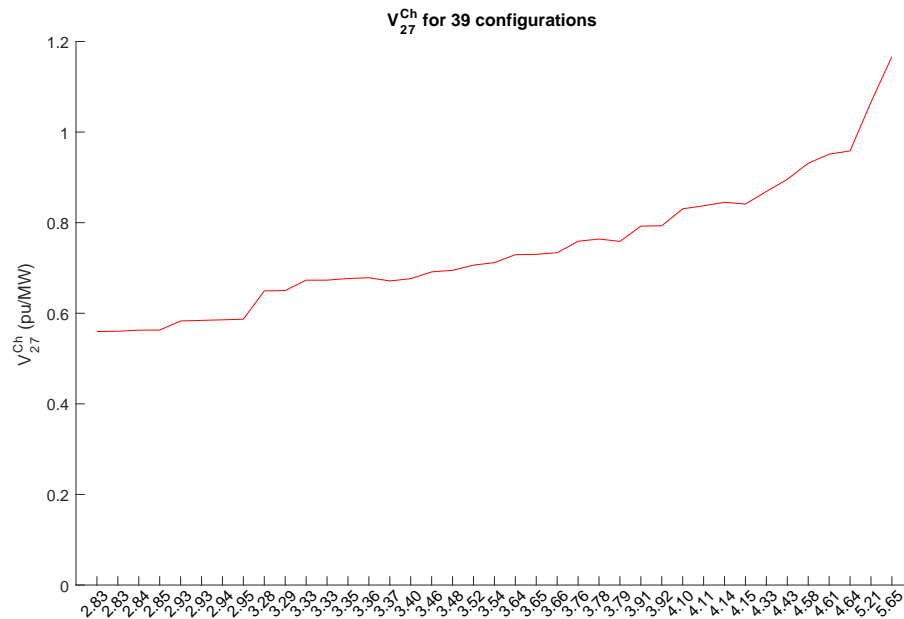

Figure 5.8: Comparing voltage changes at V_{POI} (POI=bus 27) for 39 configurations using V_{27}^{Ch}, 0.9 capacitive DG power factor

cases, i.e. [1 1 1 0 1 1 1 1], and is achieved when imposing a limit of maximum 4 allowable switch operations.
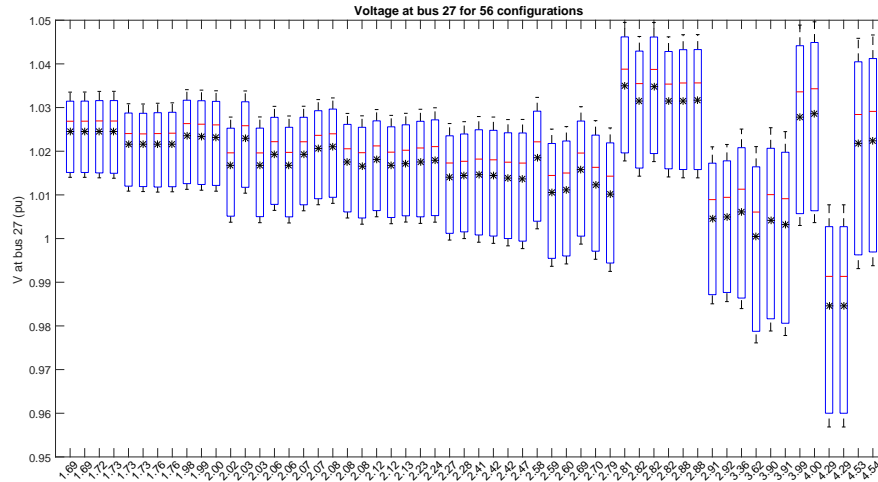

Figure 5.9: Box and Whisker plots for V_{POI} (POI=bus 27) for 56 configurations, 0.9 inductive power factor

Fig. 5.10 shows the values of V_{27}^{Ch}, which confirms that lower voltage variations is seen in inductive power factor operation of DG.
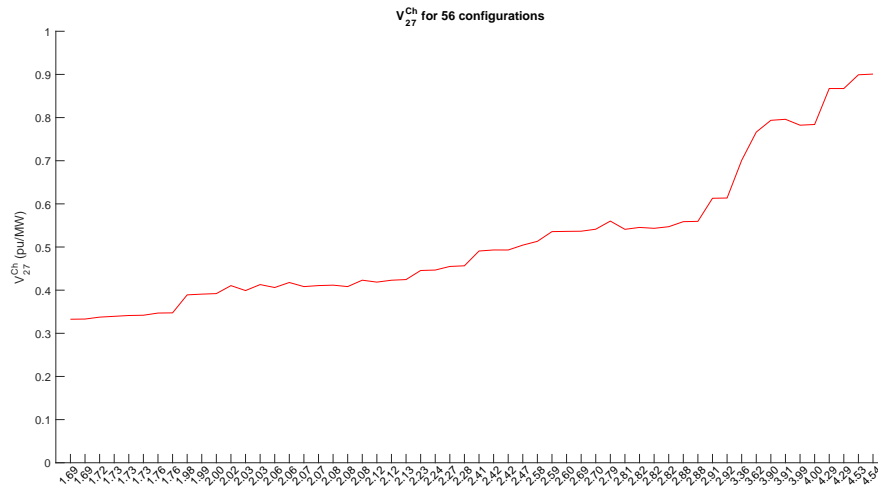

Figure 5.10: Comparing voltage changes at V_{POI} (POI=bus 27) for 56 configurations using V_{27}^{Ch}, 0.9 inductive DG power factor

5.4.4   Scenario 4: Minimizing Variations in A Remote Bus Voltage with Given DG Capacity

Using the same methodology stated in Section 5.3.2 and considering $\alpha_m = 10$ and $\alpha_{POI} = 0$ in Step 5, one can achieve the topology which allows for the desired penetration level in the selected DG power factor, and satisfies the operational constraints as well as continuity of service to all the loads, while affecting the voltage at a remote bus the least possible. For brevity, only results for unity DG power factor are provided here, while similar observations for capacitive and inductive modes can be concluded based on aforementioned statements.

Considering unity DG power factor, the same 46 configurations seen in Scenario 3 are selected, and the topology with the least value of $R_{27,12}$ is selected as the optimal configuration, i.e. the configuration in which the state of switches is [1 1 0 0 1 0 0 1].

To further analyze the results, the same renewable DG is connected to bus 27 with the output profile shown in Fig. 5.3, while the maximum value of the curve is set to 1.9 MW (50% penetration). Load flow is performed for 780 minutes of the study period, and the values of V_{12} are achieved in all 46 configurations. Fig. 5.11 presents the box plot for these values, when the configurations are sorted based on ascending order of $R_{27,12}$. As can be seen, there is very negligible change in the voltage at bus 12 in the optimum configuration. If the operator is interested in selecting a configuration with a desired number of switching operations, for example with 3 switch operations, the seventh box plot in Fig. 5.11 would be achieved, with $R_{27,12} = 0.3$, and configuration of $S =$[1 1 0 0 0 0 1 1].

Fig. 5.12 shows the values of V_{12}^{Ch}. Again, the x-axis shows the values of (5.26) for each of the configurations, and are sorted in an ascending order. As seen in this figure, the least values of (5.19) have led to lower changes in the voltage magnitude at bus 12.

Similar to Fig. 5.5, a heat plot for voltage at bus 12 for all 780 minutes of the

simulation in 46 different configurations is shown in Fig. 5.13, which again confirms the negligible variations of the voltage at bus 12.
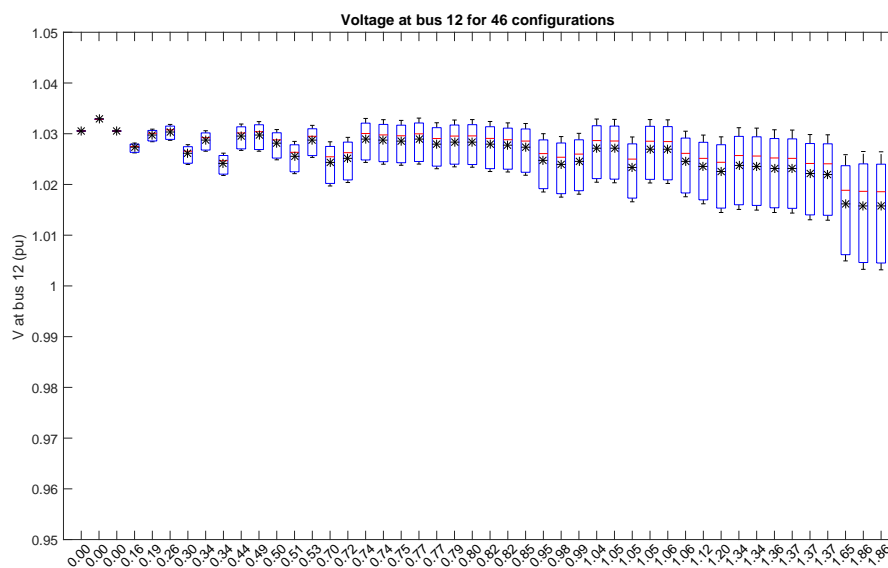

Figure 5.11: Box and Whisker plots for V_{12} (POI=bus 27) for 46 configurations, unity DG power factor
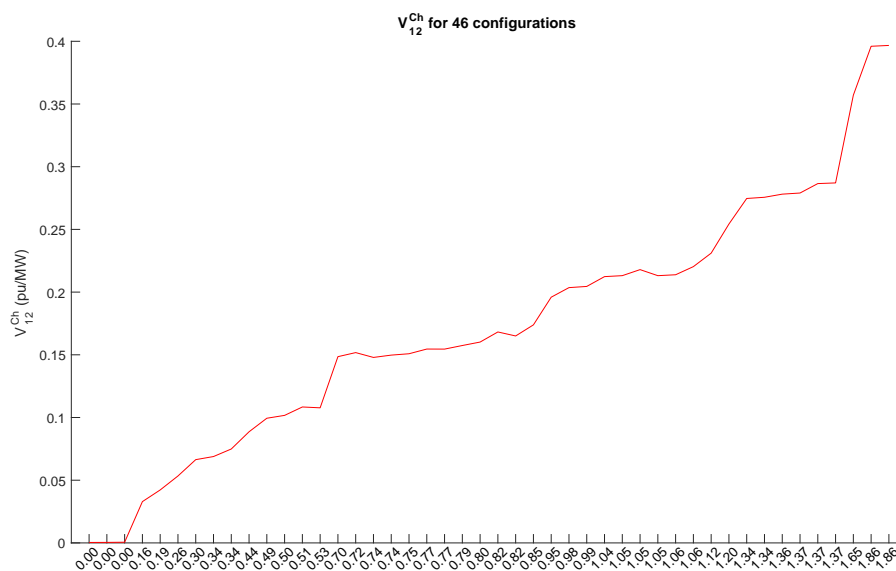
Figure 5.12: Values of V_{12}^{Ch} when POI=bus 27 for 46 configurations, unity DG power factor
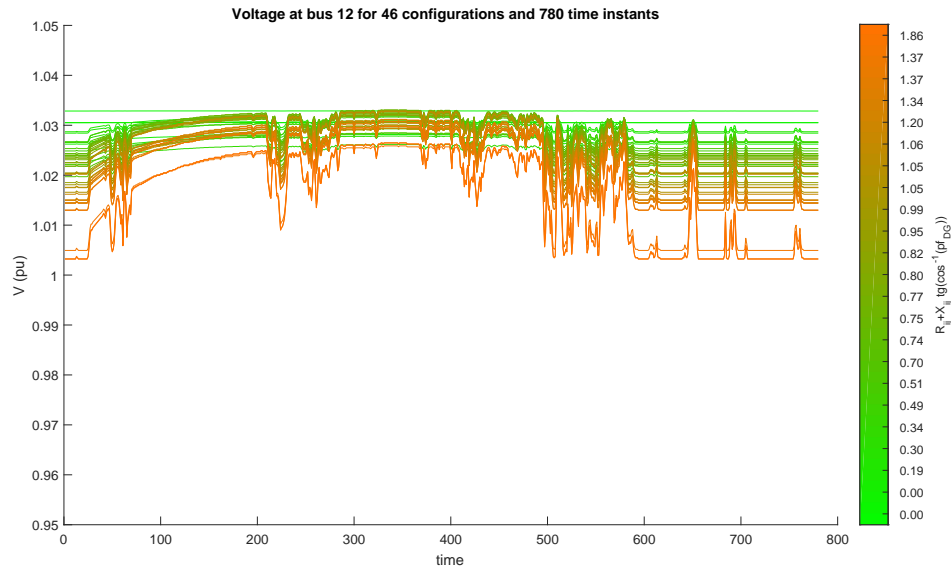
Figure 5.13: Heat plot for V_{12} (POI=bus 27) for 46 configurations

In order to see the impact of the proposed method on performance of voltage regulating devices, a voltage regulator is considered between nodes 11 and 12 with the settings provided in Table 5.4, where V_{set} is the central voltage in regulator controller in per unit and BW is the bandwidth in per unit. Note that the proposed NR scheme is capable of achieving the desired goal regardless of the regulator setting and its operation in the system.

Table 5.4: Regulator settings

From	To	Control	Tap ratio	Total taps	V_{set}	BW
11	12	Bus 12 Volt.	$\pm5\%$	32	1.025	0.015

The regulator is considered to be operating with the settings mentioned in Table 5.4. For all the 46 configurations that allow for the DG output profile with a maximum of at least 1.9 MW, load flow calculations are performed for the 780 minutes of studied period. Then, box and whisker plots of V_{12} are shown in Fig. 5.14. The upper and lower limit of voltage used by the control strategy of regulator are also shown in the plot. As shown in this figure, although the regulator has helped to maintain the

voltage at bus 12 in the desired limit of $V_{set} \pm BW$, the previous trend is still valid; i.e, the lower values of (5.19) have led to lower changes in the voltage profile of the interested bus for the study.
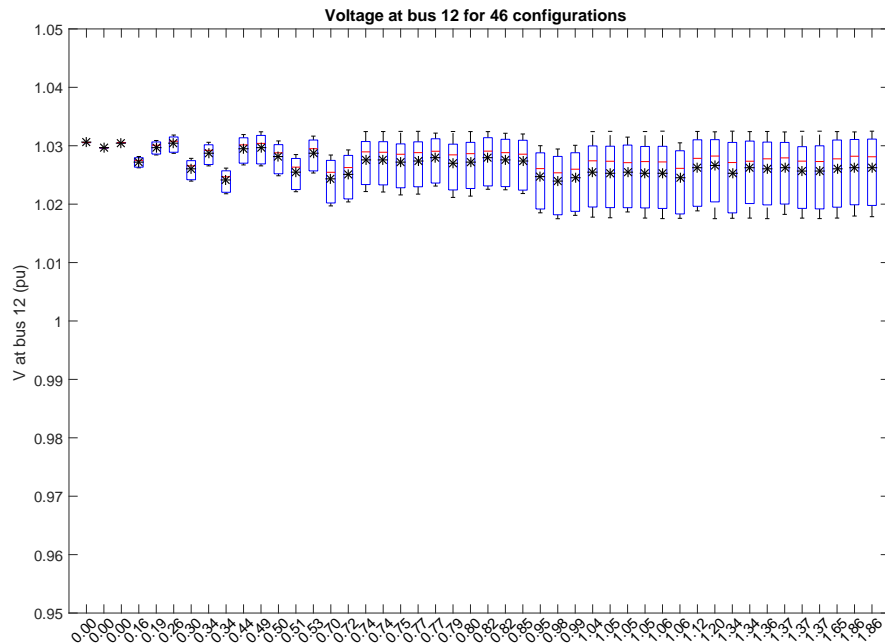

Figure 5.14: Box and Whisker plots for V_m (m=bus 12) for 46 configurations

To see the burden that voltage variations put on voltage regulators in order to keep the magnitude of V_{12} within the range of $V_{set} \pm BW$, number of regulator tap operations for the respective configuration and the same conditions described for Fig. 5.14 are presented in Fig. 5.15. As can be seen in Fig. 5.14, a lower value of (5.19) results in less variations in V_{12}, which generally leads to a lower number of regulator tap changes, as seen in Fig. 5.15. Note that due to non-linearity of the operation of regulator, in some point in the plot, the tap operation of two consecutive configurations might not follow the aforementioned trend; since in one configuration with lower value of (5.19), the changes of V_{12} over time might be in such a way that it violates the limit of $V_{set} \pm BW$ although the distribution of V_{12} seen in Fig. 5.11 or Fig. 5.14 is less than the other configuration.
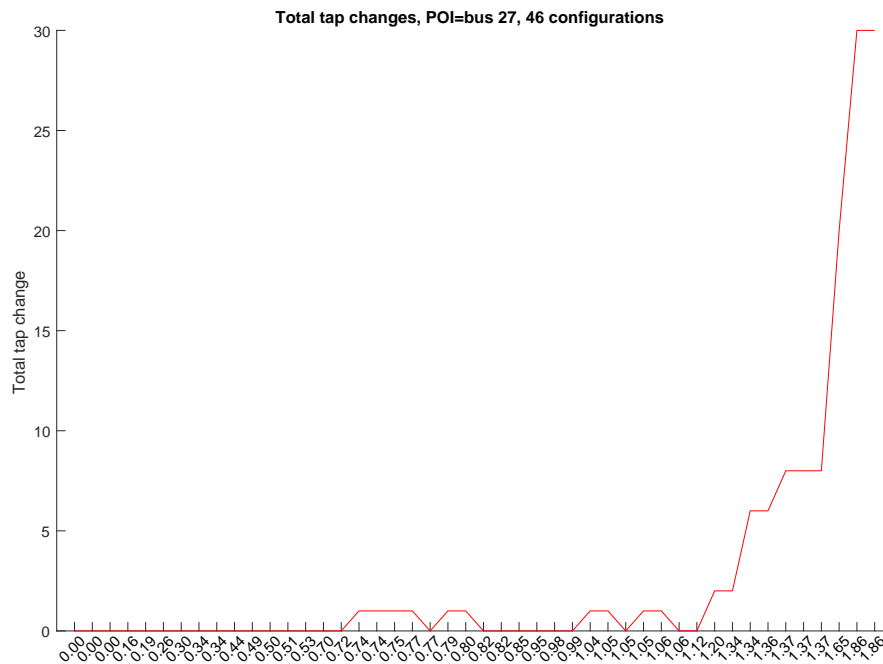
Figure 5.15: Regulator tap operations, POI= bus 27, $P^{Max} = 1.9\ MW$

5.4.5 Effect of Variable Load Profile on the Proposed Scheme

For calculating the optimum topology to achieve the desired goals while load profile is expected to change, the only requirement is having the minimum and maximum load forecast of the feeder in the study period. As stated in Chapter 3, minimum load allows for lower value of installed DG capacity. Therefore, while selecting the topologies which allow for the desired penetration level, it is required to select the minimum loading condition. Moreover, while checking the no-DG scenario for violations in voltage and current limits, maximum loading condition should be considered. After having the minimum and maximum load forecast during the study period, negligible impact of load variation is expected on the proposed scheme. This is due to the fact that since loads are considered in parallel with the distribution lines for Z_{bus} calculations, variable loads have negligible impact on the Z_{bus} elements, especially while selecting the minimum values of either Z_{th} at the POI or $Z_{POI,m}$. For verification,

load profile is changed from 10% to 100% in steps of 10%, and values of $Z_{27,27}$ and $Z_{27,12}$ are calculated for all 130 topologies whose no-DG scenario satisfies (4.4), (4.2), and (4.3). For $Z_{27,12}$, for instance, the top 18 topologies with the least values stay the same while load profile varies. Although the next rankings among all topologies varies with a variable load profile, the values of $Z_{27,12}$ stay very close.

In order to see the impact of variable load profile, load data from field measurements with resolution of 15 minutes, as seen in Fig. 5.16, are used. The minimum load value during the day, while PV is expected to generate power, is 1.98 MW and 1.37 $MVAr$, while maximum load is 3.8 MW. Note that load resolution and load profile can be changed as desired, as the NR scheme only needs the minimum and maximum load profile to be known for its calculations.
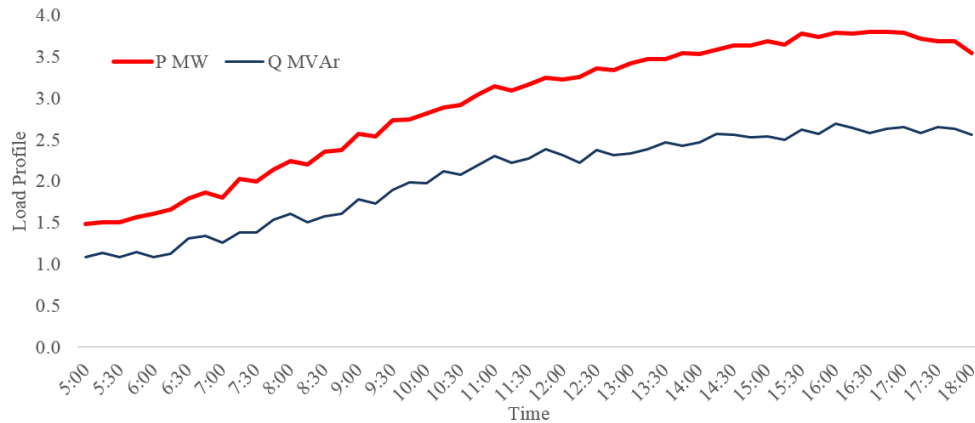
Figure 5.16: Load profile based on real measurements

DG capacity is considered 1.52 MW, which satisfies a penetration level of 40% in maximum load, and 75% based on the minimum load. The proposed NR scheme is used as follows to have the least impact on regulator tap operation, while N_{SO} is not considered. For this purpose, a total of 35 configurations satisfy the desired penetration level in the minimum day-time load, while their voltages and currents are within the limits in the maximum loading condition. Then, the configuration with the least value of $Z_{27,12}$ is selected, which is $S = [11001001]$.

In order to verify the results obtained by the proposed scheme, load flow is per-

formed for the study period, and voltage at bus 12 is shown using box plots in Fig. 5.17 for all 35 configurations. Moreover, total tap operations for all 35 configurations are shown in Fig. 5.18. As seen in these figures, the topologies with lower values of $R_{27,12}$ have shown less variations in the voltage at bus 12 as well as lower tap operations, even though load profile is considered variable as shown in Fig. 5.16.
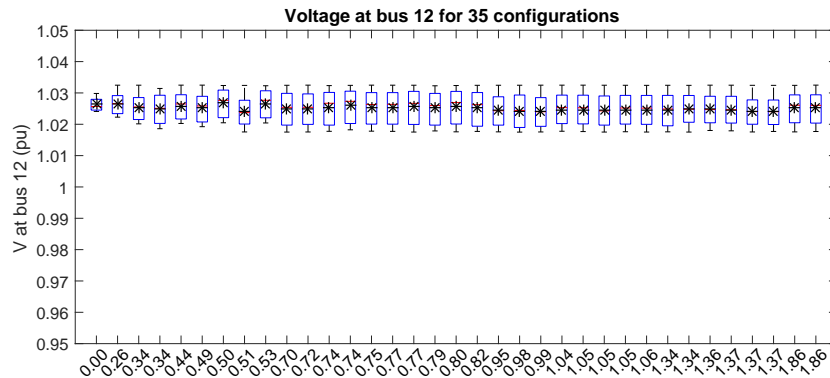
Figure 5.17: Box and Whisker plots for V_{12} for 35 configurations, considering variable load and regulator
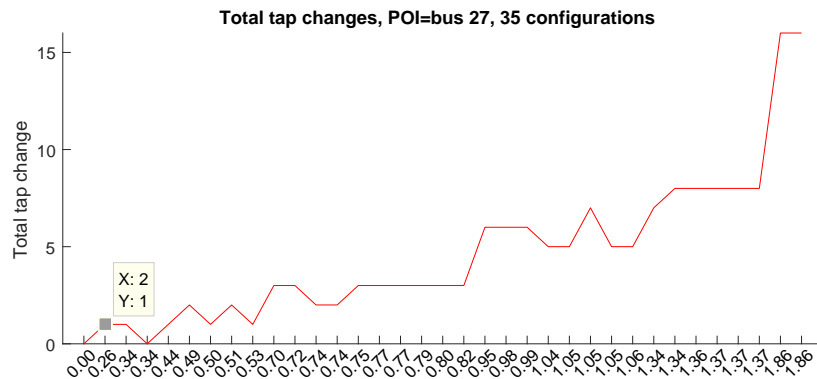
Figure 5.18: Regulator tap operations, POI= bus 27, $P^{Max} = 1.52 \ MW$

5.4.6 An Unbalanced Test Case

In previous examples, IEEE 69 bus system has been used. The proposed network reconfiguration scheme does not depend on the type of load flow program to achieve the optimum topology, and voltage plots, shown in form of box and whisker plots or heat plots, are presented only for demonstration purposes. To verify the Independence

of the proposed NR scheme from the test case and the load flow program used to present the voltage plots, the IEEE 34 node test feeder [97] is selected as test system in this part, as shown in Fig. 5.19. Voltage level is 24.9 kV, except for the path downstream the transformer at bus 832, which changes the voltage level to 4.16 kV. Capacitors are installed at buses 844 and 848, and installed capacity at each phase for these nodes are 100 kVAr and 150 kVAr, respectively. Two different meshed structures have been considered. Meshed case C_1 is formed by adding a 3 phase line (configuration 301) between nodes 852 and 840 with the length of 3 km, and C_2 is formed by adding the same line but with the length of 2.5 km between nodes 816 and 832.
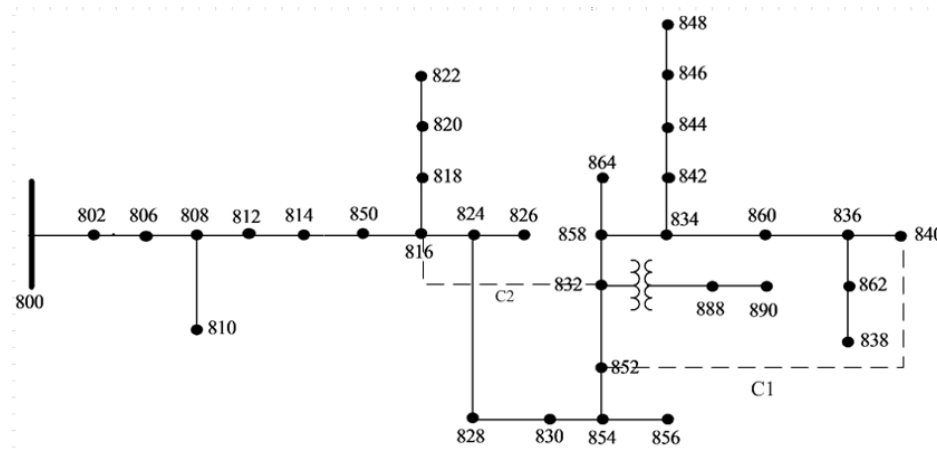
Figure 5.19: Modified IEEE 34 bus test feeder [97]

DG output is selected as shown in Fig. 5.20, based on measurement from NREL BMS location [95] on Feb 12, 2015, between noon and 1 pm, which is recorded in 1 min intervals. Since the total load of the system is 1769 kW, the maximum DG power output is selected to be 500 kW which denotes a 28% DG penetration. The DG power factor is selected to be unity for ease of comparison.

Bus 840 which is at the end of a heavy loaded branch is selected as POI. The
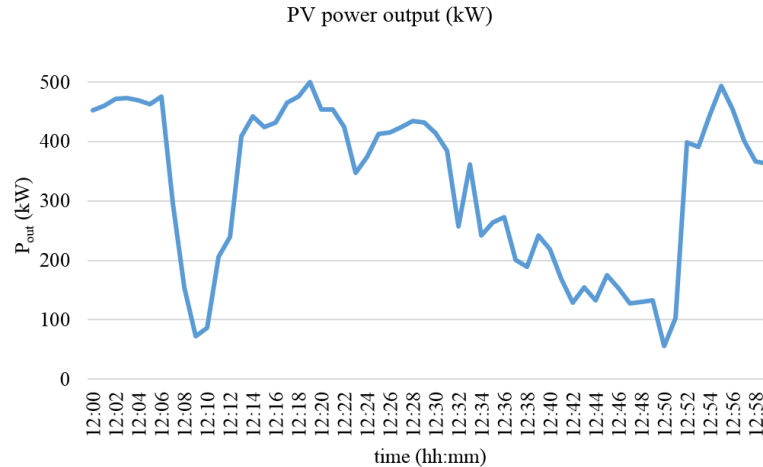
Figure 5.20: DG power output

Thevenin impedance at this bus can be calculated using (5.31):

$$|Z_{th}| = \frac{|V_{OC}|}{|I_{SC}|} \tag{5.31}$$

where $|V_{OC}|$ is the open circuit voltage at the bus (i.e the voltage at the bus when no load or generation is connected to the bus) and $|I_{SC}|$ is the solid short-circuit current at the bus. Due to the unbalanced nature if the test case, the values presented here are the positive sequence of symmetrical components domain.

The positive sequence $|Z_{th}|$ values at the POI in radial as well as meshed configurations C_1 and C_2 are seen in Table 5.5. Meshed configurations C_1 and C_2 affect the Z_{th} value in comparison with the radial configuration significantly. Therefore, it is excepted to see less voltage variations at the POI due to DG variable output in both meshed scenarios in comparison with the radial configuration.

Table 5.5: Positive sequence $|Z_{th}|$ values at bus 840 in radial and select meshed structures

	radial	C_1	C_2
$|Z_{th_{840}}|$ (Ω)	0.431	0.408	0.299

In order to validate the results, the CYMDIST package of the CYME software is used. When DG is connected at bus 840, the positive sequence of voltage at bus 840

varies as a result. Fig. 5.21 shows bus 840 positive sequence voltage in C_1 and C_2 scenarios with respect to the radial case.
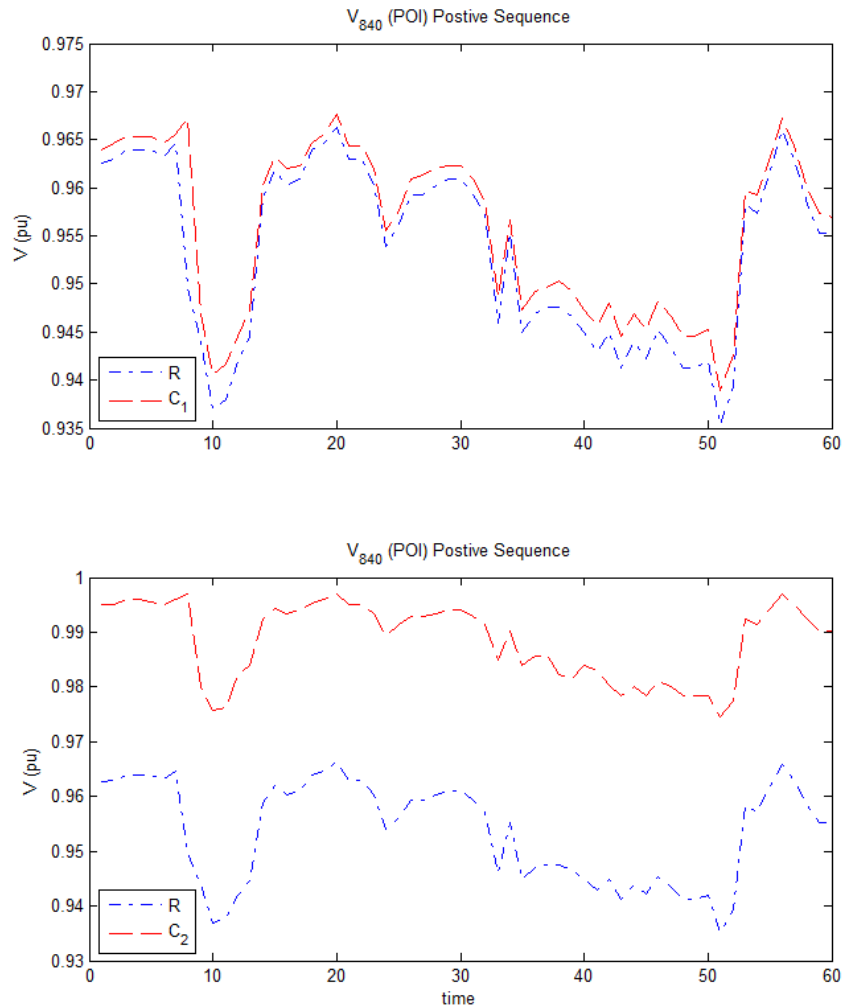
Figure 5.21: Positive sequence voltage at bus 840 between 12:00 and 13:00

For better comparison, Table 5.6 summarizes the results for the case of having DG at bus 840. One row shows the voltage span, V^{Span}, which is the difference between maximum and minimum voltage at bus 840 seen during the study period. V^{Span} can be calculated for each bus using:

$$V_i^{Span} = V_i^{Max} - V_i^{min} \tag{5.32}$$

Table 5.6: Results with DG at bus 840

	radial	C_1	C_2
V_{840}^{Span} (p.u.)	0.0310	0.0287	0.0223
V_{840}^{Ch} (p.u.)	0.1927	0.1810	0.1393

The other row shows V_{840}^{Ch} (5.30). As expected, it can be seen from Table 5.6 and Fig. 5.21 that the voltage at the POI has less variations due to the same amount of DG variation in meshed configuration C_2. Moreover, meshed configuration C_1 has better performance than the radial configuration.

As seen in the results presented in this chapter, by using the proposed NR approach, higher presence of renewable DG in DS can be achieved with the least impact on bus voltage variations. The next chapter presents the concluding remarks, a summary of research contributions, and a vision for future work.

CHAPTER 6: CONCLUSION

6.1   Overview

In this chapter, conclusion of the work is presented. First, concluding remarks on the proposed framework and the observations based on the achieved results are discussed. Then, the research contributions are summarized and reviewed. Finally, a vision on the future research direction is presented and can be based for expansion of the proposed methodologies and insights discussed in the current work.

6.2   Concluding Remarks

The work presented in this dissertation addresses the problem of proliferation of renewable distributed generation in distribution systems. The main means to achieve higher allowable penetration of distributed generation in the proposed framework is network reconfiguration, with relaxed radiality constraint, allowing to investigate both radial and meshed topologies. The proposed scheme takes into account limiting factors of steady-state voltage and current operating limits. Moreover, special attention is given to the impacts of renewable resources intermittency and variability on distribution systems bus voltage variations.

In developing the proposed network reconfiguration scheme, attention is paid to the bus impedance matrix, which is found to play an important role in the relationship between DG power variations and bus voltage changes. More specifically, the Thevenin's impedance seen at the DG point of interconnection and the off-diagonal element of bus impedance matrix relating the DG POI and a remote bus of interest are found to play an important role in how variable renewable DG profile can affect bus voltage variations. Therefore, these values are incorporated into the presented

network reconfiguration scheme. Through evaluation of the developed network re-configuration scheme, the impact of Thevenin's impedance seen at the DG point of interconnection on voltage variations is validated. As expected, creating meshes in the distribution system topology is shown to generally reduce the value of Thevenin's impedance, and to allow for higher penetration levels of renewable generation with lower negative impacts on voltage profile. Also, based on the similar relationship between variations in voltage of a remote bus and changes in distributed generation output, as expected, simulation results show significant reduction of voltage regulator operations using the presented scheme.

By following the presented network reconfiguration scheme, the maximum allowable DG capacity can be achieved with minimum impact on bus voltage variations due to variable DG output. In calculating the optimum topology to achieve the desired goals in a given time frame, the presented NR scheme considers the minimum and maximum daytime load of the distribution system in that time period as input. Therefore, calculation of the optimum solution is performed from a planning perspective, for example, daily, weekly, or monthly. However, the optimum topology introduced by this approach is robust to variations in load and distributed generation, i.e. the calculated optimum solution is valid throughout the whole time-frame, and hence it will benefit the distribution system from operation perspective as well.

6.3   Summary of Research Contributions

The main contributions of this dissertation can be summarized as follows:

- A method is developed to estimate the maximum allowable DG output in the system considering steady-state voltage and current limits. The presented method is then used to investigate the ability of meshed configuration for integrating more distributed generation to the system. In this part of the work:

  - The presented method uses only one iteration of power flow to determine

the maximum DG capacity considering both voltage and current limits.

– Using the presented sensitivity-based method, maximum allowable DG capacity based on steady-state current and voltage limits is compared in radial and different meshed configurations. Results have shown that meshed configuration can allow for higher DG capacity in DS.

– It is found that the impact of meshed configuration on maximum allowable DG capacity is different for each bus. Hence, selective meshed configuration is suggested as a solution for increased DG penetration.

– Impact of loading conditions and DG power factors are also investigated, and results of these observations are also used in the continuation of the work in next parts.

• As the first step of the work revealed, there is a need to select the optimum topology to allow for highest possible DG capacity at a certain bus of interest. Therefore, an optimization problem is formulated to find the DS configuration with highest penetration level of distributed generation, considering steady-state voltage and current limits, with decision variables being size of the DG and the system topology. In this work, the following discussions are made:

– An optimization problem is formulated as a generalized solution to allow for maximum installed DG capacity.

– The radiality constraint is relaxed and the network reconfiguration problem is formulated such that both radial and meshed configurations are considered.

– Steady-state bus voltage and line current limits are considered as constraints.

– Superior behavior of select meshed configurations is seen in terms of increased hosting capacity of the distribution system.

- Increased capacity of DG also requires mitigation measures for the negative impacts of variable and intermittent renewable DG power output. In the third part of the work, special attention is given to intermittent and variable renewable distributed generation and its negative impact on bus voltage variations. In this part of the work:

  - The relationship between power variations of renewable distributed generation and changes seen in bus voltage profile is investigated.

  - Stiffness factor of DS at the POI, which is inversely proportional to the Thevenin impedance seen at POI, is found to be a governing factor in the above relationship.

  - In case of having a bus with sensitive voltage, relationship between variations of distributed generation output and voltage at that bus is found to be impacted by the off-diagonal element of bus impedance matrix, related to the POI and the bus of interest.

  - In order to select the optimum DS configuration allowing for highest DG rated capacity with minimum impact on bus voltage variations, the Thevenin impedance at DG point of interconnection and the off-diagonal element of the bus impedance matrix relating DG POI and the bus of interest are incorporated in the network reconfiguration problem.

  - Results have shown that meshed configuration can provide the goal of increasing DG integration, and also reducing the voltage profile variations while integrating renewable distributed generation. This in turn leads to improved operation of DS, such as less voltage regulator tap operations.

6.4   Future Work and Vision

Several suggestions and comments can be made in terms of future vision for the work presented in this dissertation. Ideas for additions and improvements to the

proposed work include:

- Requirements for updating the protection system can be considered in the presented network reconfiguration scheme. Although conventional protection schemes are not applicable in meshed topologies, choosing the most appropriate scheme in terms of cost or technical aspects can be considered while moving from radial to meshed configurations.

- Utility practices with meshed configurations have justified cost of upgrading protection system moving from radial feeders to meshed topologies considering only reliability improvements. A cost benefit analysis can be performed, not only considering the required upgrades in the protection system, but also the benefits of reduced voltage regulator operations, reduced switching operations compared with other techniques, and increased penetration of renewable sources.

- Results of a similar cost benefit study can be used to select the most appropriate feeder to perform the proposed network reconfiguration scheme among a set of candidate feeders. This can include several factors studied in this dissertation, such as percentage of improvements in distributed generation installed capacity from radial to meshed topology, ratio of minimum load to maximum load for the feeder, presence of voltage sensitive nodes in the feeder, current protection scheme of the feeder, etc.

- Harmonic distortion in presence of renewable distributed generation is investigated in the literature. Findings of this dissertation can be used to analyze the harmonic distortion in case of radial and meshed configurations. Most importantly, since meshed configuration has shown to generally increase the stiffness factor at the DG point of interconnection, this topology can be utilized to reduce the share of harmonic currents from inverter-based renewable distributed

generation into the system.

- In this dissertation, location of the switches has been assumed constant. A switch placement problem could be formulated to select the best place to form the mesh, i.e. the best location of the tie-switch, or the best place to have the sectionalizing switches. This could be utilized in designing new distribution systems as well as upgrading the existing systems.

REFERENCES

[1] W. H. Kersting, *Distribution system modeling and analysis*. CRC press, 2012.

[2] A. J. Pansini, *Electrical distribution engineering*. Fairmont Press, 2007.

[3] C. Penuela Meneses and J. Sanches Mantovani, "Improving the grid operation and reliability cost of distribution systems with dispersed generation," *Power Systems, IEEE Transactions on*, vol. 28, no. 3, pp. 2485–2496, Aug 2013.

[4] M. Biglarbegian, B. Vatani, I. Mazhari, and B. Parkhideh, "Thermal storage capacity to enhance network flexibility in dual demand side management," in *2015 North American Power Symposium (NAPS)*, Oct 2015, pp. 1–5.

[5] M. Al-Muhaini and G. T. Heydt, "Evaluating future power distribution system reliability including distributed generation," *Power Delivery, IEEE Transactions on*, vol. 28, no. 4, pp. 2264–2272, 2013.

[6] S. Moghadasi and S. Kamalasadan, "Optimal fast control and scheduling of power distribution system using integrated receding horizon control and convex conic programming," *IEEE Transactions on Industry Applications*, vol. 52, no. 3, pp. 2596–2606, May 2016.

[7] A. Heidari, V. G. Agelidis, H. Zayandehroodi, J. Pou, and J. Aghaei, "On exploring potential reliability gains under islanding operation of distributed generation," *IEEE Transactions on Smart Grid*, vol. 7, no. 5, pp. 2166–2174, Sept 2016.

[8] A. Heidari, V. G. Agelidis, M. Kia, J. Pou, J. Aghaei, M. Shafie-Khah, and J. P. S. Catalão, "Reliability optimization of automated distribution networks with probability customer interruption cost model in the presence of dg units," *IEEE Transactions on Smart Grid*, vol. 8, no. 1, pp. 305–315, Jan 2017.

[9] I.-K. Song, W.-W. Jung, J.-Y. Kim, S.-Y. Yun, J.-H. Choi, and S.-J. Ahn, "Operation schemes of smart distribution networks with distributed energy resources for loss reduction and service restoration," *Smart Grid, IEEE Transactions on*, vol. 4, no. 1, pp. 367–374, 2013.

[10] K. Mahmoud, N. Yorino, and A. Ahmed, "Optimal distributed generation allocation in distribution systems for loss minimization," *IEEE Transactions on Power Systems*, vol. 31, no. 2, pp. 960–969, March 2016.

[11] M. H. J. Bollen and F. Hassan, *Integration of Distributed Generation in the Power Systems*. IEEE Press, 2011.

[12] E. Karatepe, F. Ugranlı, and T. Hiyama, "Comparison of single-and multiple-distributed generation concepts in terms of power loss, voltage profile, and line flows under uncertain scenarios," *Renewable and Sustainable Energy Reviews*, vol. 48, pp. 317–327, 2015.

[13] V. Mendez, J. Rivier, J. De La Fuente, T. Gomez, J. Arceluz, J. Marin, and A. Madurga, "Impact of distributed generation on distribution investment deferral," *International Journal of Electrical Power & Energy Systems*, vol. 28, no. 4, pp. 244–252, 2006.

[14] A. J. Lamadrid, D. L. Shawhan, C. E. M.-S. . nchez, R. D. Zimmerman, Y. Zhu, D. J. Tylavsky, A. G. Kindle, and Z. Dar, "Stochastically optimized, carbon-reducing dispatch of storage, generation, and loads," *IEEE Transactions on Power Systems*, vol. 30, no. 2, pp. 1064–1075, March 2015.

[15] Z. Ding and W.-J. Lee, "A stochastic microgrid operation scheme to balance between system reliability and greenhouse gas emission," in *Industrial & Commercial Power Systems Technical Conference (I&CPS), 2015 IEEE/IAS 51st*. IEEE, 2015, pp. 1–9.

[16] J. Morren and S. de Haan, "Maximum penetration level of distributed generation without violating voltage limits," in *SmartGrids for Distribution, 2008. IET-CIRED. CIRED Seminar*, June 2008, pp. 1–4.

[17] J. Agüero, "Improving the efficiency of power distribution systems through technical and non-technical losses reduction," in *Transmission and Distribution Conference and Exposition (T&D), 2012 IEEE PES*, May 2012, pp. 1–8.

[18] I. N. Santos, V. Ćuk, P. M. Almeida, M. H. Bollen, and P. F. Ribeiro, "Considerations on hosting capacity for harmonic distortions on transmission and distribution systems," *Electric Power Systems Research*, vol. 119, pp. 199–206, 2015.

[19] J. Agüero and S. Steffel, "Integration challenges of photovoltaic distributed generation on power distribution systems," in *Power and Energy Society General Meeting, 2011 IEEE*, July 2011, pp. 1–6.

[20] S. Eftekharnejad, V. Vittal, G. T. Heydt, B. Keel, and J. Loehr, "Impact of increased penetration of photovoltaic generation on power systems," *Power Systems, IEEE Transactions on*, vol. 28, no. 2, pp. 893–901, 2013.

[21] H. Ayres, W. Freitas, M. de Almeida, and L. da Silva, "Method for determining the maximum allowable penetration level of distributed generation without steady-state voltage violations," *Generation, Transmission Distribution, IET*, vol. 4, no. 4, pp. 495–508, April 2010.

[22] W. Sheng, S. Zhao, X. Song, and X. Meng, "Maximum penetration level of distributed generation in consideration of voltage fluctuations based on multi-resolution model," *Generation, Transmission Distribution, IET*, vol. 9, no. 3, pp. 241–248, 2015.

[23] M. Baran, H. Hooshyar, Z. Shen, and A. Huang, "Accommodating high PV penetration on distribution feeders," *Smart Grid, IEEE Transactions on*, vol. 3, no. 2, pp. 1039–1046, June 2012.

[24] P. Barker, "Distributed solar integration experiences," in *Distributed Wind/Solar Interconnection Workshop.* Utility Variable-Generation Integration Group (UVIG), May 2013.

[25] P. Pachanapan, A. Dysko, O. Anaya-Lara, and K. Lo, "Harmonic mitigation in distribution networks with high penetration of converter-connected dg," in *PowerTech, 2011 IEEE Trondheim*, June 2011, pp. 1–6.

[26] V. Khadkikar, R. K. Varma, R. Seethapathy, A. Chandra, and H. Zeineldin, "Impact of distributed generation penetration on grid current harmonics considering non-linear loads," in *Power Electronics for Distributed Generation Systems (PEDG), 2012 3rd IEEE International Symposium on.* IEEE, 2012, pp. 608–614.

[27] A. Bhowmik, A. Maitra, S. Halpin, and J. Schatz, "Determination of allowable penetration levels of distributed generation resources based on harmonic limit considerations," *Power Delivery, IEEE Transactions on*, vol. 18, no. 2, pp. 619–624, April 2003.

[28] K. Rahimi, S. Mohajeryami, and A. Majzoobi, "Effects of photovoltaic systems on power quality," in *North American Power Symposium (NAPS), 2016.* IEEE, 2016, pp. 1–6.

[29] *Assessment of Demand-Side Resources within the Eastern Interconnection*, 2013, navigant Consulting Inc. [Online]. Available: http://www.naruc.org/grants/ Documents/Assessment%20of%20Demand%20Side%20Resources%20within% 20EISPC%20-%20Final%20Report%20March%202013%20Revised%20(2)1.pdf

[30] "Stochastic analysis to determine feeder hosting capacity for distributed solar PV systems," EPRI, Palo Alto, CA: 2012. 1026640.

[31] M. Rylander, J. Smith, and W. Sunderman, "Streamlined method for determining distribution system hosting capacity," *IEEE Transactions on Industry Applications*, vol. 52, no. 1, pp. 105–111, Jan 2016.

[32] E. Sáiz-Marán, E. Lobato, and I. Egido, "Local hosting capacity increase by means of wind farm voltage control provision," *IEEE Transactions on Power Systems*, vol. 29, no. 4, pp. 1731–1738, July 2014.

[33] D. Cheng, B. A. Mather, R. Seguin, J. Hambrick, and R. P. Broadwater, "Photovoltaic (pv) impact assessment for very high penetration levels," *IEEE Journal of Photovoltaics*, vol. 6, no. 1, pp. 295–300, Jan 2016.

[34] F. Capitanescu, L. F. Ochoa, H. Margossian, and N. D. Hatziargyriou, "Assessing the potential of network reconfiguration to improve distributed generation hosting capacity in active distribution systems," *IEEE Transactions on Power Systems*, vol. 30, no. 1, pp. 346–356, Jan 2015.

[35] M. R. Dorostkar-Ghamsari, M. Fotuhi-Firuzabad, M. Lehtonen, and A. Safdarian, "Value of distribution network reconfiguration in presence of renewable energy resources," *IEEE Transactions on Power Systems*, vol. 31, no. 3, pp. 1879–1888, May 2016.

[36] A. M. Eldurssi and R. M. O'Connell, "A fast nondominated sorting guided genetic algorithm for multi-objective power distribution system reconfiguration problem," *IEEE Transactions on Power Systems*, vol. 30, no. 2, pp. 593–601, March 2015.

[37] H. Ahmadi and J. R. Martã, "Minimum-loss network reconfiguration: A minimum spanning tree problem," *Sustainable Energy, Grids and Networks*, vol. 1, pp. 1 – 9, 2015.

[38] C. Lee, C. Liu, S. Mehrotra, and Z. Bie, "Robust distribution network reconfiguration," *IEEE Transactions on Smart Grid*, vol. 6, no. 2, pp. 836–842, March 2015.

[39] A. Asrari, S. Lotfifard, and M. S. Payam, "Pareto dominance-based multiobjective optimization method for distribution network reconfiguration," *IEEE Transactions on Smart Grid*, vol. 7, no. 3, pp. 1401–1410, May 2016.

[40] A. Asrari, T. Wu, and S. Lotfifard, "The impacts of distributed energy sources on distribution network reconfiguration," *IEEE Transactions on Energy Conversion*, vol. 31, no. 2, pp. 606–613, June 2016.

[41] F. Ding and K. A. Loparo, "Hierarchical decentralized network reconfiguration for smart distribution systems part I: Problem formulation and algorithm development," *IEEE Transactions on Power Systems*, vol. 30, no. 2, pp. 734–743, March 2015.

[42] P. M. de Quevedo, J. Contreras, M. J. Rider, and J. Allahdadian, "Contingency assessment and network reconfiguration in distribution grids including wind power and energy storage," *IEEE Transactions on Sustainable Energy*, vol. 6, no. 4, pp. 1524–1533, Oct 2015.

[43] A. Asrari, S. Lotfifard, and M. Ansari, "Reconfiguration of smart distribution systems with time varying loads using parallel computing," *IEEE Transactions on Smart Grid*, vol. 7, no. 6, pp. 2713–2723, Nov 2016.

[44] S. R. Tuladhar, J. G. Singh, and W. Ongsakul, "Multi-objective approach for distribution network reconfiguration with optimal dg power factor using nspso," *IET Generation, Transmission Distribution*, vol. 10, no. 12, pp. 2842–2851, 2016.

[45] S. F. Santos, D. Z. Fitiwi, M. R. Cruz, C. M. Cabrita, and J. P. Catalão, "Impacts of optimal energy storage deployment and network reconfiguration on renewable integration level in distribution systems," *Applied Energy*, vol. 185, pp. 44–55, 2017.

[46] V. Cecchi, X. Yang, K. Miu, and C. Nwankpa, "Instrumentation and measurement of a power distribution system laboratory for meter placement and network reconfiguration studies," *Instrumentation Measurement Magazine, IEEE*, vol. 10, no. 5, pp. 10–19, October 2007.

[47] K. Miu, H.-D. Chiang, and R. McNulty, "Multi-tier service restoration through network reconfiguration and capacitor control for large-scale radial distribution networks," *Power Systems, IEEE Transactions on*, vol. 15, no. 3, pp. 1001–1007, Aug 2000.

[48] D. Halamay, M. Antonishen, K. Lajoie, A. Bostrom, and T. K. A. Brekken, "Improving wind farm dispatchability using model predictive control for optimal operation of grid-scale energy storage," *Energies*, vol. 7, no. 9, p. 5847, 2014. [Online]. Available: http://www.mdpi.com/1996-1073/7/9/5847

[49] Y. Zhang, Z. Y. Dong, F. Luo, Y. Zheng, K. Meng, and K. P. Wong, "Optimal allocation of battery energy storage systems in distribution networks with high wind power penetration," *IET Renewable Power Generation*, vol. 10, no. 8, pp. 1105–1113, 2016.

[50] K. Rahimi and B. Chowdhury, "A hybrid approach to improve the resiliency of the power distribution system," in *North American Power Symposium (NAPS), 2014*, Sept 2014, pp. 1–6.

[51] S. Teleke, M. Baran, A. Huang, S. Bhattacharya, and L. Anderson, "Control strategies for battery energy storage for wind farm dispatching," *Energy Conversion, IEEE Transactions on*, vol. 24, no. 3, pp. 725–732, Sept 2009.

[52] I. Naziri Moghaddam and B. Chowdhury, "Optimal sizing of hybrid energy storage systems to mitigate wind power fluctuations," in *Power Energy Society General Meeting, 2016 IEEE*, 2016, pp. 1–5.

[53] L. Wenxia, N. Shuya, and X. Huiting, "Optimal planning of battery energy storage considering reliability benefit and operation strategy in active distribution system," *Journal of Modern Power Systems and Clean Energy*, pp. 1–10, 2010.

[54] C. Hill, M. Such, D. Chen, J. Gonzalez, and W. Grady, "Battery energy storage for enabling integration of distributed solar power generation," *Smart Grid, IEEE Transactions on*, vol. 3, no. 2, pp. 850–857, June 2012.

[55] S. N. Salih, P. Chen, O. Carlson, and L. B. Tjernberg, "Optimizing wind power hosting capacity of distribution systems using cost benefit analysis," *IEEE Transactions on Power Delivery*, vol. 29, no. 3, pp. 1436–1445, June 2014.

[56] A. Rabiee and S. M. Mohseni-Bonab, "Maximizing hosting capacity of renewable energy sources in distribution networks: A multi-objective and scenario-based approach," *Energy*, 2016.

[57] L. Collins and J. Ward, "Real and reactive power control of distributed PV inverters for overvoltage prevention and increased renewable generation hosting capacity," *Renewable Energy*, vol. 81, pp. 464–471, 2015.

[58] H. Jafarian, J. Enslin, and B. Parkhideh, "On reactive power injection control of distributed grid-tied ac-stacked pv inverter architecture," in *Energy Conversion Congress and Exposition (ECCE), Milwaukee*, 2016.

[59] Y. Guangya, F. Marra, M. Juamperez, S. B. Kjaer, S. Hashemi, J. Østergaard, H. H. Ipsen, and K. H. Frederiksen, "Voltage rise mitigation for solar pv integration at lv grids," *Journal of Modern Power Systems and Clean Energy*, vol. 3, no. 3, pp. 411–421, 2015.

[60] F. Harirchi, M. G. Simoes, M. Babakmehr, A. Al-Durra, and S. M. Muyeen, "Designing smart inverter with unified controller and smooth transition between grid-connected and islanding modes for microgrid application," in *2015 IEEE Industry Applications Society Annual Meeting*, Oct 2015, pp. 1–7.

[61] H. Jafarian, M. Biglarbegian, and B. Parkhideh, "Controller robustness analysis of grid-tied AC-stacked PV inverter system considering manufacturing inaccuracies," in *Applied Power Electronics Conference and Exposition (APEC), 2017 IEEE*, 2017.

[62] B. Mather, "NREL/SCE high-penetration PV integration project: Report on field demonstration of advanced inverter functionality in Fontana, CA," 2014.

[63] B. Pagel, "Energizing international drive," *Transmission & Distribution World*, vol. 52, no. 4, p. 18, 2000.

[64] R. P. Fanning, "Implementation of networked primary and secondary distribution systems for us utilities," in *2003 IEEE Power Engineering Society General Meeting (IEEE Cat. No.03CH37491)*, vol. 4, July 2003, p. 2429 Vol. 4.

[65] R. Fanning and R. Huber, "Distribution vision 2010: planning for automation," in *IEEE Power Engineering Society General Meeting, 2005*, June 2005, pp. 2614–2615 Vol. 3.

[66] A. Nikander, S. Repo, and P. Järventausta, "Utilizing the ring operation mode of medium voltage distribution feeders," in *Proc of 17th International Conference on Electricity Distribution*, 2003.

[67] T.-H. Chen, W.-T. Huang, J.-C. Gu, G.-C. Pu, Y.-F. Hsu, and T.-Y. Guo, "Feasibility study of upgrading primary feeders from radial and open-loop to normally closed-loop arrangement," *Power Systems, IEEE Transactions on*, vol. 19, no. 3, pp. 1308–1316, Aug 2004.

[68] W. T. Huang and S. T. Chen, "Line loss reduction by distribution system upgrading from radial to normally closed-loop arrangement," in *2009 Ninth International Conference on Hybrid Intelligent Systems*, vol. 3, Aug 2009, pp. 334–339.

[69] G. Celli, F. Pilo, G. Pisano, V. Allegranza, R. Cicoria, and A. Iaria, "Meshed vs. radial MV distribution network in presence of large amount of DG," in *Power Systems Conference and Exposition, 2004. IEEE PES*, Oct 2004, pp. 709–714 vol.2.

[70] M. C. Alvarez-Herault, D. Picault, R. Caire, B. Raison, N. HadjSaid, and W. Bienia, "A novel hybrid network architecture to increase dg insertion in electrical distribution systems," *IEEE Transactions on Power Systems*, vol. 26, no. 2, pp. 905–914, May 2011.

[71] P. C. Chen, R. Salcedo, Q. Zhu, F. de Leon, D. Czarkowski, Z. P. Jiang, V. Spitsa, Z. Zabar, and R. E. Uosef, "Analysis of voltage profile problems due to the penetration of distributed generation in low-voltage secondary distribution networks," *IEEE Transactions on Power Delivery*, vol. 27, no. 4, pp. 2020–2028, Oct 2012.

[72] J.-C. GU, K.-Y. SHEN, and W. LIAO, "Performance assessment for normally closed-loop type distribution power systems," in *International Conference on Power Systems (7th WSEAS), PE*, vol. 7, 2007, pp. 138–145.

[73] B. Ruben, A. Cross, D. Strickland, M. Aten, and R. Ferris, "Meshing radial networks at 11kv," in *2011 2nd IEEE PES International Conference and Exhibition on Innovative Smart Grid Technologies*, Dec 2011, pp. 1–8.

[74] "Overview of Con Edison system and LIC network," in *Con Edison*, January 2010.

[75] T.-H. Chen, E.-H. Lin, N.-C. Yang, and T.-Y. Hsieh, "Multi-objective optimization for upgrading primary feeders with distributed generators from normally closed loop to mesh arrangement," *International Journal of Electrical Power & Energy Systems*, vol. 45, no. 1, pp. 413–419, 2013.

[76] S. Riverso, F. Sarzo, and G. Ferrari-Trecate, "Plug-and-play voltage and frequency control of islanded microgrids with meshed topology," *IEEE Transactions on Smart Grid*, vol. 6, no. 3, pp. 1176–1184, May 2015.

[77] L. Che, X. Zhang, M. Shahidehpour, A. Alabdulwahab, and Y. Al-Turki, "Optimal planning of loop-based microgrid topology," *IEEE Transactions on Smart Grid*, vol. PP, no. 99, pp. 1–11, 2016.

[78] J. R. Fairman, K. Zimmerman, J. W. Gregory, and J. K. Niemira, "International drive distribution automation and protection," in *27th Annual Western Protective Relay Conference, Spokane, WA*, 2000.

[79] K.-Y. Shen and J.-C. Gu, "Protection coordination analysis of closed-loop distribution system," in *Proceedings. International Conference on Power System Technology*, vol. 2, 2002, pp. 702–706 vol.2.

[80] R. J. Yinger, S. S. Venkata, and V. A. Centeno, "Southern california edison's advanced distribution protection demonstrations," *IEEE Transactions on Smart Grid*, vol. 3, no. 2, pp. 1012–1019, June 2012.

[81] F. A. Viawan, D. Karlsson, A. Sannino, and J. Daalder, "Protection scheme for meshed distribution systems with high penetration of distributed generation," in *2006 Power Systems Advanced Metering, Protection, Control, Communication, and Distributed Resources*, March 2006, pp. 99–104.

[82] F. A. Viawan and D. Karlsson, "Various protection schemes for closed loop feeders with synchronous machine based distributed generation and their impacts on reliability," in *2007 IEEE Lausanne Power Tech*, July 2007, pp. 1170–1175.

[83] B. Li, X. Yu, and Z. Bo, "Protection schemes for closed loop distribution network with distributed generator," in *2009 International Conference on Sustainable Power Generation and Supply*, April 2009, pp. 1–6.

[84] A. Prasai, Y. Du, A. Paquette, E. Buck, R. Harley, and D. Divan, "Protection of meshed microgrids with communication overlay," in *2010 IEEE Energy Conversion Congress and Exposition*, Sept 2010, pp. 64–71.

[85] M.-C. Alvarez-Herault, N. N' Doye, C. Gandioli, N. Hadjsaid, and P. Tixador, "Meshed distribution network vs reinforcement to increase the distributed generation connection," *Sustainable Energy, Grids and Networks*, pp. 20 – 27, 2015.

[86] H. H. Zeineldin, H. M. Sharaf, D. K. Ibrahim, and E. E. D. A. El-Zahab, "Optimal protection coordination for meshed distribution systems with dg using dual setting directional over-current relays," *IEEE Transactions on Smart Grid*, vol. 6, no. 1, pp. 115–123, Jan 2015.

[87] J. Downey, "Duke Energy compromises on new requirement that threatened to curtail solar projects," http://www.bizjournals.com/charlotte/news/2016/08/30/duke-energy-compromiseson-new-requirement-that.html, visited 2017-01-03.

[88] H. Saadat, *Power system analysis.* McGraw-Hill Primis Custom, 2002.

[89] M. Baran and F. Wu, "Optimal capacitor placement on radial distribution systems," *Power Delivery, IEEE Transactions on*, vol. 4, no. 1, pp. 725–734, Jan 1989.

[90] J. Savier and D. Das, "Impact of network reconfiguration on loss allocation of radial distribution systems," *Power Delivery, IEEE Transactions on*, vol. 22, no. 4, pp. 2473–2480, Oct 2007.

[91] R. J. Wilson and J. J. Watkins, *Graphs: an introductory approach–a first course in discrete mathematics.* Wiley New York, 1990.

[92] D. Goldberg, "Genetic algorithms in search, optimization, and machine learning," *Addion Wesley*, vol. 1989, 1989.

[93] M. M. Begovic, I. Kim, D. Novosel, J. R. Aguero, and A. Rohatgi, "Integration of photovoltaic distributed generation in the power distribution grid," in *System Science (HICSS), 2012 45th Hawaii International Conference on*, Jan 2012, pp. 1977–1986.

[94] "IEEE application guide for IEEE std 1547(TM), IEEE standard for interconnecting distributed resources with electric power systems," *IEEE Std 1547.2-2008*, pp. 1–217, April 2009.

[95] "Solar calendars," National Reneable Energy Laboratory (NREL), Measurement and Instrumentation Data Center (MIDC). [Online]. Available: http://www.nrel.gov/midc

[96] B. Mather, B. Kroposki, R. Neal, F. Katiraei, A. Yazdani, J. R. Aguero, T. E. Hoff, B. L. Norris, A. Parkins, R. Seguin *et al.*, "Southern california edison high-penetration photovoltaic project–year," *Contract*, vol. 303, pp. 275–3000, 2011.

[97] W. Kersting, "Radial distribution test feeders," in *Power Engineering Society Winter Meeting, 2001. IEEE*, vol. 2, 2001, pp. 908–912.